THE
PHYSICAL REVIEW
A journal of experimental and theoretical physics established by E. L. Nichols in 1893

SECOND SERIES, VOL. 68, NOS. 5 AND 6 · SEPTEMBER 1 AND 15, 1945

Researches on the Magnetic Deflection of the Hard Component of Cosmic Rays*

G. BERNARDINI, M. CONVERSI, E. PANCINI, E. SCROCCO, AND G. C. WICK
Istituto di Fisica dell'Universita di Roma, Rome, Italy

(Received August 4, 1945)

The energy spectrum and positive excess of the hard component of cosmic rays have been investigated both in Rome (50 m above sea level) and at Pian Rosà (3500 m above sea level) by means of a counter system with deflecting magnetized cores. The results of several measurements are discussed, and the following interpretation is suggested: (1) A positive excess of the order of 20 percent is found in the hard component, in agreement with the results of other investigators. (2) The hypothesis of the existence of several types of mesons is not confirmed in the lower atmosphere (between 0 and 5000 m). (3) Assuming for the ratio $\tau/\mu c^2$ between the meson proper lifetime τ and the rest energy μc^2 the value $\tau/\mu c^2 = 3\times10^{-6}$ sec./Mev, one has to assume that the energy spectrum of mesons at the top of the atmosphere does not follow a power law $E^{-2.9}$ for low values of the energy ($E<4\times10^9$ ev).

1. INTRODUCTION

IN the years 1941–43 we have performed in the Physical Institute of the University of Rome a number of experiments on the mesonic component of cosmic rays by means of magnetized iron cores. We present here an outline of this work: some details that will be omitted may be found elsewhere.[1]

The first attempts to detect the deflection of cosmic particles by the magnetic field in an iron core were made in 1930 by Rossi[2] and Mott-Smith[3] independently. Their apparatus were rather different, but similar in two respects: both used a counter telescope to detect the particles, and in both cases the effect investigated was essentially a differential one, depending on the charged particles in the radiation being of one sign only or, at least, prevalently so.

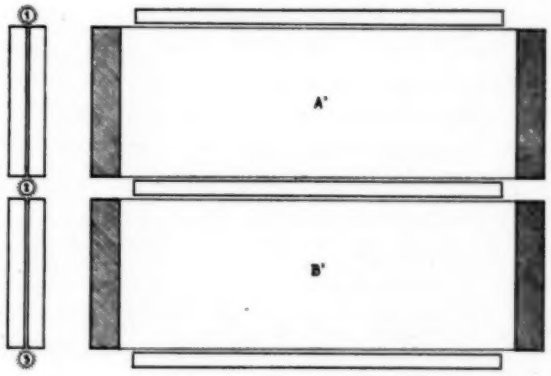

FIG. 1. Arrangement of counters and magnetic cores.

* A fund for researches on cosmic rays was granted by the Consiglio Nazionale delle Ricerche.

[1] G. Bernardini and M. Conversi, La Ric. Scient. **11**, 858 (1940). G. Bernardini, M. Conversi, E. Pancini, and G. C. Wick, La Ric. Scient. **12**, 1227 (1941). M. Conversi and E. Scrocco, N. Cim. **I**, 372 (1943); Bernardini, Conversi, Pancini, and Wick, Phys. Rev. **60**, 535 (1941).

[2] B. Rossi, Nature **128**, 300 (1931).

[3] L. M. Mott-Smith, Phys. Rev. **35**, 1125 (1930); **37**, 1001 (1931); **39**, 403 (1932).

FIG. 2. Coils of pair of cores ($A'A''$ or $B'B''$).

Mott-Smith obtained a negative result.[4] Rossi on the other hand, by means of a telescope consisting of only two counters found an indication of a small effect, corresponding to an excess of the positive over the negative particles; the evidence, however, was partly contradictory and was not regarded as definite by the author.

Looking at these results in the light of later knowledge we can see that: (a) the hypothesis that the effective field inside iron is not given by the induction vector B and is considerably smaller than B (this, of course, would easily explain the negative result of the deflection experiments of Mott-Smith and Rossi) has been dismissed by a theoretical discussion by v. Weizsäcker;[5] (b) an alternative explanation is offered by Blackett's result,[6] namely that the radiation consists of positive and negative particles in approximately equal numbers; (c) while this is probably the correct explanation, we must not forget that there is a certain discrepancy between Blackett's statement and the subsequent investigations of Leprince-Ringuet and Crussard,[7] Jones,[8] and Hughes.[9] Especially the last two authors have given quite definite evidence of the existence of a small but real excess in the number of the positive over the negative mesons; the excess is of the order of 20 percent, and according to this, one should find in an experiment like that of Rossi a small but definite effect.

It would seem, therefore, that the subject deserves further investigation; but there are more cogent reasons too. The positive excess in the meson spectrum is probably connected with the positive nature of the primary radiation that is revealed by the azimuthal effect;[10] a study of the variation of the positive excess with height would probably be interesting and might throw some light on the process of creation of the mesons. Now the Wilson chamber method

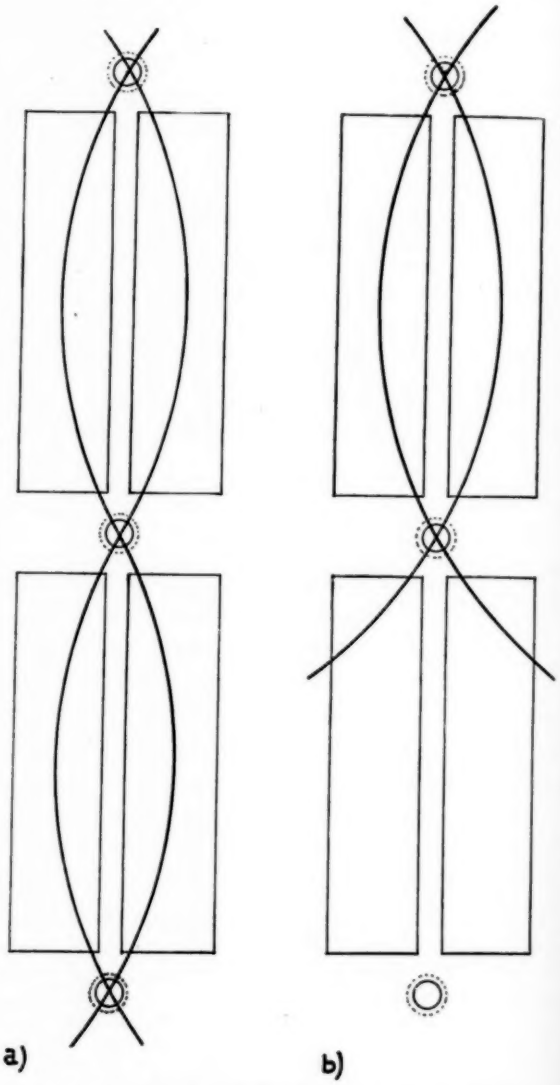

FIG. 3. Qualitative shape of trajectories: (a) "cc" arrangement; (b) "cd" arrangement.

[4] In a subsequent investigation, however, Danforth and Swann, Phys. Rev. **49**, 582 (1936) have found a small but real effect by means of an apparatus not very different from that of Mott-Smith.

[5] C. F. Weizsäcker, Ann. d. Physik **17**, 869 (1933).

[6] P. S. M. Blackett, Proc. Roy. Soc. **159**, 1 (1937).

[7] L. Leprince Ringuet and J. Crussard, J. de. Phys. **8**, 207 (1937).

[8] H. Jones, Rev. Mod. Phys. **11**, 235 (1939).

[9] D. J. Hughes, Phys. Rev. **57**, 592 (1940).

[10] T. H. Johnson, Rev. Mod. Phys. **11**, 208 (1939).

employed by all the authors mentioned above is obviously unsuitable for this purpose owing to the rather heavy equipment it requires.

Bearing this in mind, we have tried to improve Rossi's experiment, and we have planned an apparatus consisting of a triple coincidence system with four iron cores; we have found that it gives a quite measurable effect, depending upon the positive excess. We hope to use it for an investigation of the positive excess in the upper atmosphere.

This apparatus also allows an entirely different use since the magnetization of the cores can be arranged in such a way as to cause a deflection effect which is not differential. That is, the effect depends on the energy of the particles, but not on their sign; accordingly, we have found in this case a substantially larger effect, which can be used for investigation of the energy spectrum of the particles.[11]

2. APPARATUS

Our apparatus is shown schematically in Fig. 1; it consists primarily of three coincident counters having a radius $r=1$ cm and useful length of about 50 cm. The distance d between the axis of the intermediate counter "2" and that of either counter "1" or "3" is 22 cm. The two pairs of iron cores A', A'' and B', B'' are magnetized by coils as is shown by Fig. 2. The field in the cores is parallel to the axis of the counters and has opposite directions in A', A'' (similarly in B' B''). The magnetic circuit is closed by iron bars applied at both ends of A', A'' (or B', B''). Thus each pair of iron cores, for instance A', A'', acts, roughly speaking, like a cylindrical magnetic lens which concentrates the particles of one sign. We shall hence-forward speak of this "lens" as convergent (or briefly "c") or divergent (briefly "d") for positive ($c+$ or $d+$) or negative ($c-$ or $d-$) particles.

[11] The main results of the present paper have already been indicated in a preliminary communication (Phys. Rev. reference 1). After the present paper was completed we have learned from a private communication that F. Rasetti has recently succeeded in obtaining a deflection effect by an arrangement of the type used by Mott-Smith. His results are in accord with the theoretical prediction that the effective field inside iron is B and with the existence of a positive excess. All this seems to be in the best agreement with our own previous conclusions and with these of the present paper.

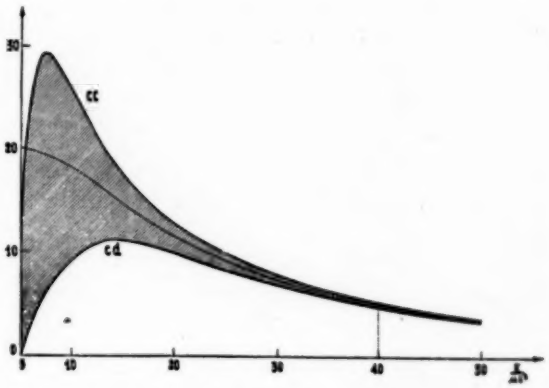

FIG. 4. Modification impressed upon the total energy spectrum (positive+negative mesons) by the action of the instrument with either arrangement "*cc*" or "*cd*."

Now the upper (A', A'') and lower (B', B'') pairs can be magnetized in the same way or not, so that on the whole we have the following *four* possibilities:

$$cc+\ (=dd-);\quad dd+\ (=cc-);$$
$$cd+\ (=dc-);\quad dc+\ (=cd-).$$

The two alternatives *cc* and *cd* are schematically shown in Fig. 3.

With the "*cc*" arrangement, the number of positive particles detected by the counter telescope is increased, the number of the negative particles is decreased, and the reverse takes place with the "*dd*" arrangement. The difference $N_{cc+}-N_{cc-}$ between the number of triple coincidences, N_{cc+} or N_{cc-} registered in a given time with the two arrangements depends on the asymmetry of the meson spectrum; *it may be used to measure the positive excess*, as a more quantitative analysis will show.

We shall later develop a theory of the action of the instrument. Figure 4 gives an idea of the modification impressed upon the total energy spectrum (positives+negatives) by the action of the magnetic lenses with either arrangement *cc* or *cd*. In this case the positive excess has been neglected; the broken line in Fig. 4 shows the energy spectrum at sea level in the vertical direction and in open air. This spectrum has been evaluated by assuming, as usual, a power spectrum for the mesons at the creation level in the upper atmosphere, and by taking into account the disintegration of the mesons, and by assuming for the mean lifetime of τ of a

TABLE I. Measurements of the positive excess.

Meters above sea level	$10^{-3}B$ (gauss)	Threefold coinc./hour N_{cc+}	Threefold coinc./hour N_{cc-}	Double coinc./hour N_{c+}	Double coinc./hour N_{c-}	δ	δ'
50 (Roma)	2.4	81.1±1.2	77.7±1.2	235.4±2.4	234.4±2.3	4.3±2.1	0.4±1.4
	5.0	83.1±1.2	77.2±1.1	243.6±2.4	235.7±2.3	7.4±2.0	3.3±1.4
	10.4	88.5±0.9	80.5±0.9	245.2±1.9	236.2±1.8	9.5±1.5	3.7±1.1
	15.5	97.5±1.0	84.7±0.9	253.7±2.0	242.3±1.9	14.0±1.5	4.6±1.1
	17.0	103.3±1.5	91.2±1.3	260.2±2.8	250.5±2.5	12.4±2.0	3.8±1.5
3500 (Pian Rosà)	2.4	170.0±2.1	175.0±2.2	615±8.0	601±8.0	1.1±1.7	2.3±1.9
	5.0	180.5±2.5	172.0±2.5	597±9.5	589±9.5	4.8±2.0	1.3±2.3
	10.4	190.5±2.1	174.5±2.0	609±4.5	583±4.5	8.8±1.6	4.4±1.1
	15.5	221.0±1.8	191.0±2.0	664±4.0	624±4.0	14.6±1.3	6.2±0.9
	17.0	223.0±2.7	200.0±2.9	678±7.5	631±7.5	15.2±1.8	7.2±1.6

meson a value:[12] $\tau/\mu c^2=2\times10^{-8}$ sec./Mev (μ is the meson mass) with $\mu c^2=100$ Mev.

The full lines give the spectrum as modified by the field (and the absorption in the iron cores) when the field B in the two pairs of iron coils is $B=17{,}000$ gauss. It can be seen that the spectrum is noticeably modified in the energy interval, between 5×10^8 ev—the minimum energy for a meson to get through the iron bars—and 4×10^9 ev. The spectrum becomes richer in low energy particles with the *cc* arrangement; the reverse takes place with the *cd*, or *dc*, arrangement.

One can see, also that the energy range of field sensitive particles is about the same as for the Wilson chamber technique.[13]

The Wilson chamber, of course, allows a much more detailed analysis of the energy spectrum to be made, but this advantage is attained only by the much greater labor which the method requires.

On the whole we think that the two methods are not mutually exclusive, but that they can usefully integrate each other.

3. RESULTS

(a) The Positive Excess

These measurements were made partly in the Physical Institute of the University of Rome and partly at Pian Rosà (Cervinia) 3500 m above sea level in a wooden hut.[14]

During the measurements the two arrangements *cc*+ and *cc*− were, of course, systematically alternated; also, several values of the magnetic field were tested. The electric pulses of counters were sent to a coincidence system which registered besides the triple coincidences also the double coincidences between the two upper counters.

[12] This value of $\tau/\mu c^2$ is, in our opinion, rather too low; but we have chosen it in our calculation because it is intermediate between the several values found by different experiments.

[13] In comparing the sensitivity of our apparatus with that attained in the Wilson chamber, it is well to remember that in the latter case the limit to the measurement of large energies is not set by the difficulty of measuring the small curvatures involved, but rather by the spurious curvatures produced by irregular motions of the chamber gas. In our case this cause of error does not exist; unfortunately, it is superseded to a certain extent by a similar effect due to scattering of the mesons in the iron cores. This causes a spurious curvature of the trajectories, and thus tends to obscure the effect of the magnetic field. The following evaluation shows, however, that the change in the action of the magnetic "lens" by the scattering, must not be very large (and, at any rate, the spurious curvatures due to scattering vary as the reciprocal of the particle energy; that is, they become smaller at the same rate as the true curvatures, which is not the case in the Wilson chamber!).

The order of magnitude of the spurious curvatures introduced by scattering can be evaluated by means of Williams' formulae, Proc. Roy. Soc. **169**, 531 (1939), which give the mean deflection $\bar{\vartheta}$ suffered by a particle in going through a plate of thickness t, of atomic number Z, density ρ, atomic weight A. Consider, for instance, a particle moving in a plane normal to the axis of the counters and call θ the component of the deflection parallel to this plane—this is in fact the component in which we are mainly interested, as it is indistinguishable from a deflection due to the magnetic field—we find, according to Williams:

$$\bar{\vartheta}=\sim\frac{600Ze(Nt)^{\frac{1}{2}}}{\beta E}\left[3.7+0.28\log\frac{Z^{4/3}\rho t}{A\beta^2}\right],$$

where E is the energy of the particle in e-volts, βc its velocity ($\beta\approx1$), and N is the number of atoms per cm³. In iron we find: $\bar{\vartheta}=\sim((\sqrt{t})/E)10^7$, when $t\approx20$ up to 40 cm.

The deflection caused by the magnetic field is: $\vartheta'=300Bt/E$, which becomes, when $B=15000$ gauss: $\vartheta'=(t/E)10^6$. Putting $t=40$ cm, one can see that ϑ' is about three times as large as $\bar{\vartheta}$, independently of energy.

[14] A series of measurements in a plane flying at 9000 m above sea level was also begun, but unfortunately a flying accident destroyed the apparatus before a sufficient set of data had been secured.

These could be compared with Rossi's results, although the distance between the counters and the counter diameter are not quite the same. Our results are shown in Table I.

The effect δ in the sixth column is defined by:

$$\delta = 200 \frac{N_{cc+} - N_{cc-}}{N_{cc+} + N_{cc-}}. \qquad (1)$$

The effect δ' in the seventh column is defined in a similar way for the double coincidences.

The value of δ has been evaluated without taking into account the effect of *showers*, which had been shown in the usual way (that is by shifting the upper counter horizontally, out of the solid angle defined by the remaining two counters) to be negligible.

The correction for random coincidences is negligible in the case of the triple ones; the double coincidences due to chance were about 40/hr. at Pian Rosà as well as in Rome[15] and they are already taken account of in the N_{c+} and N_{c-} values given in Table I.

In Figs. 5 and 6, the values of δ and δ', found in Rome and at Pian Rosà, are plotted against the field B. The effect on double coincidences, δ', is seen to be quite a bit smaller than on δ; this is understandable since doubling the distance between the extreme counters not only increases the angular definition of the beam selected by the telescope, but also doubles the deflection caused by the field. In fact, the theory of the apparatus (Section 4) shows that the sensitivity increases, roughly, with the square of the distance between the counters.

Whatever the reason may be, the effect δ' which we have found with the double coincidences is much less reliable than δ.

Considering the values of δ found at Rome and Pian Rosà, one can see that the results are quite similar, indicating that the positive excess in the meson spectrum does not materially change between sea level and 3500 meters.

With regard to the dependence of δ on B, one may remark that δ can never be larger than the positive excess ϵ, if ϵ is distributed uniformly over the energy spectrum. Indeed one can see that δ would finally become equal to ϵ if the action of the "lenses" would become strong enough to exclude the particles of one sign completely. The $\delta(B)$ curve should therefore resemble a saturation curve. But with the field values we have reached, there is no indication of a bend. Our results, however, are not inconsistent with the hypothesis that for higher values of B, δ might tend to a saturation value.

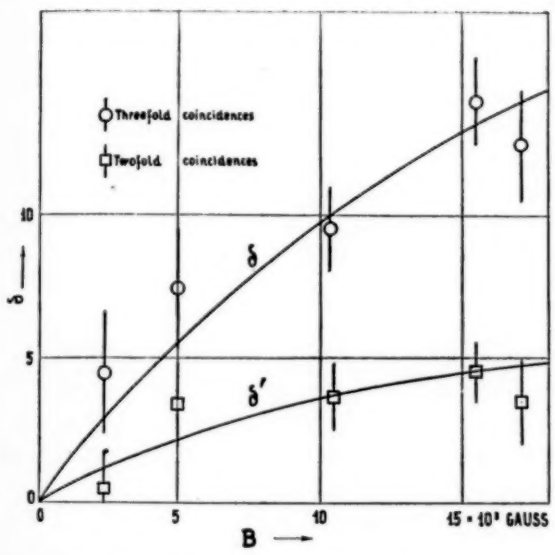

FIG. 5. Results of the measurements of the positive excess performed in Rome (50 m above sea level).

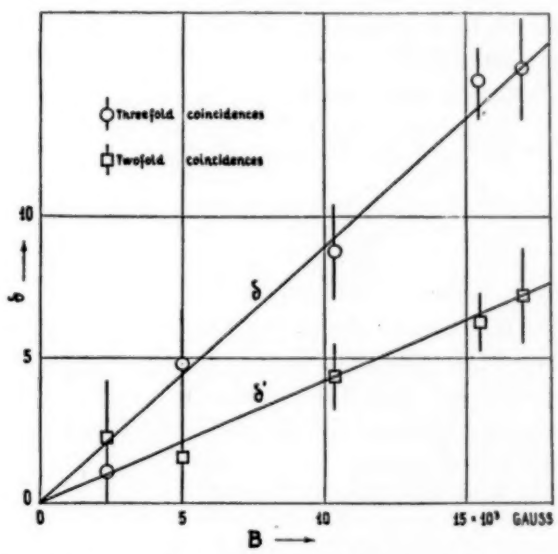

FIG. 6. Results of the measurements of the positive excess performed at Pian Rosà (3500 m above sea level).

[15] The building material of the Institute is weakly radioactive and increases the natural pulses of counters.

TABLE II. Measurements on the meson energy spectrum ($B=17{,}000$ gauss).

Series	Meters above sea level	Absorbing layer (g/cm²)	Arrangement	Threefold coincidences per hour ($N_{cc\pm}$; $N_{cd\pm}$)	$\alpha\pm$	α	$\Delta=\alpha_+-\alpha_-$
1st	50 (Roma)	0	$cc+$	104.0±1.4	50.8±3.0	42.3±2.0	16.1±3.9
			$cd+$	69.6±1.0			
			$cc-$	94.6±1.2	34.7±2.5		
			$cd-$	70.7±0.9			
2nd	50 (Roma)	250	$cc+$	91.9±1.4	48.0±3.3	40.0±2.3	15.8±4.6
			$cd+$	62.7±1.0			
			$cc-$	80.0±1.4	32.2±2.2		
			$cd-$	61.0±1.0			
3rd	3500 (Pian Rosà)	0	$cc+$	233.7±3.8	67.2±4.5		
			$cd+$	145.6±2.7			

(b) Measurements of the Meson Energy Spectrum

The results of these measurements, Table II, are grouped in three separate series, each series comprising measurements made at the same height above sea level and with the same absorber thickness above the apparatus.

In the first two series of measurements, made in Rome, the direction of the current was systematically changed in the coils around $A'A''$ and independently in the coils around $B'B''$, so that all four arrangements $cc+$, $cc-$, $cd+$, $cd-$ were alternated.

With the mean values

$$N_{cc}=\tfrac{1}{2}[N_{cc+}+N_{cc-}];\quad N_{cd}=\tfrac{1}{2}[N_{cd+}+N_{cd-}],\quad (2)$$

the effect we were looking for was defined by

$$\alpha=100(N_{cc}-N_{cd})/N_{cd}. \quad (3)$$

This is given in the next to the last column of Table II. In the third series (at Pian Rosà 3500 m above sea level) the current in the $A'A''$ coils was never changed so that the upper "lens" was always convergent for positive particles. The effect was, therefore, defined by

$$\alpha_+=100(N_{cc+}-N_{cd+})/N_{cd+}. \quad (4)$$

The second series of measurements was planned after Nielsen, Ryerson, Nordheim, and Morgan[16] had announced that a new careful investigation of the proper lifetime of a meson had given a value $\tau/\mu c^2=1.25\times10^{-8}$ sec./Mev, considerably lower than all values previously found.

With this value one can see that the maximum in the energy spectrum of the mesons arriving at sea level in the vertical direction should lie above the minimum energy of the mesons which are not stopped in the 40 cm Fe of our apparatus. Now if a thick absorber is placed above the counter telescope, it will cut off the lower part of the energy spectrum; for a properly chosen thickness of the absorber one can see that the resulting spectrum—that is the spectrum impinging on the apparatus as modified by the absorber—is appreciably *softer* than the unmodified spectrum.

We might then expect the effect α to be increased; this is also confirmed by the more detailed considerations of Section 5. Accordingly we built a brick wall, under which our apparatus could be placed, covering the solid angle defined by the counter telescope.

The vertical thickness of the wall was 250 g/cm², and the results are grouped in the second series.

The effect of showers has been deducted from

[16] W. M. Nielsen, C. M. Ryerson, L. W. Nordheim, and K. Z. Morgan, Phys. Rev. **59**, 547 (1941).

the results included in the first two columns of Table II; the correction was, however, very small. The data given in the last column can be used for a further evaluation of the positive excess.

4. THEORY OF THE INSTRUMENT

We shall now try to draw from the experimental data a quantitative evaluation of the positive excess as well as some more detailed information about the meson spectrum.

The direction of motion of an incoming particle shall be specified by the polar angles ϑ (colatitude) and φ (longitude). As polar axis we chose the axis of a counter, or the direction of the magnetic field inside the cores. Let further $\varphi=0$ indicate the vertical plane containing the three counter axes. Put

$$dn=J(E,\vartheta,\varphi)\sin\vartheta d\vartheta d\varphi dE,$$

for the number of incoming particles per second and per cm², of energy E within the interval dE, and of direction ϑ, φ within the solid angle $\sin\vartheta d\vartheta d\varphi$.

For particles of a given sign, there must be a "cross section" of the instrument $\Sigma(E,\vartheta,\varphi)$ such that the number dN of incoming particles within the specified intervals of energy and direction, that cross the useful volume of the three counters, is given by

$$dN=dn\sum(E,\vartheta,\varphi).$$

Naturally Σ depends also on the field B, on the geometrical constants of the instrument, and on the field "arrangement" (whether *cc*, or *cd*, etc.).

Since the instrument is sensitive (or $\Sigma\neq 0$) only to particles with $|\varphi|\ll 1$ we may neglect the dependence of J on φ and use for the total number of mesons crossing the counter system

$$N=\int\int J(E,\vartheta)dE\sin\vartheta d\vartheta\int\sum(E,\vartheta,\varphi)d\varphi. \quad (5)$$

Now a more detailed investigation[17] shows that the second integral can be put in the form

$$\int\sum(E,\vartheta,\varphi)d\varphi=\psi_1(\vartheta)f(\sigma,\gamma), \quad (6)$$

where σ and γ are dimensionless measures for the energy E and the stopping power L of iron, respectively,

$$\sigma=\frac{r\cdot\sin\vartheta}{d^2Be}E;\quad \gamma=\frac{r}{dBe}L. \quad (7)$$

Here d is the distance between the axis of the central counter and either the lower or the upper counter, r is the radius of a counter, e is the charge of the particle. In Eq. (6) ψ_1 is a simple function which needs not to be known exactly; the function $f(\sigma,\gamma)$ shall be indicated as the "characteristic function" of the instrument and expresses the dependence of the cross section on all parameters involved through the relation (7).

We shall now suppose that the dependence of the spectrum $J(E,\vartheta)$ on energy and ϑ can be separated so that we can put

$$J(E,\vartheta)=\psi_2(\vartheta)\Phi(\sigma). \quad (8)$$

This hypothesis can be justified approximately; remember that the intensity of mesons of energy E, incident under a zenith angle ζ, is well represented[18] by the formula

$$\left[E+\frac{m}{\cos\zeta}\right]^{-n}dE, \quad (9)$$

with a proper choice of the constants m and n. Now since in our measurements the counter telescope was vertical, and remembering that $|\varphi|\ll 1$, we have: $\cos\zeta\approx\sin\vartheta$ and putting

$$a=\frac{d^2Be}{r}=\frac{Ld}{\gamma};\quad \psi_2(\vartheta)=\sin^n\vartheta;$$
$$\Phi(\sigma)=(a\sigma+m)^{-n}, \quad (10)$$

we really find formula (8).

Substituting (6) and (8) into (5) and integrating over ϑ, we find

$$N=\int\Phi(\sigma)f(\sigma,\gamma)d\sigma, \quad (11)$$

neglecting a constant factor which is unessential in the following development.

We have termed f the characteristic function, but in fact, there are four such functions, corre-

[17] Bernardini, Conversi, Pancini, and Wick, reference 1.

[18] Conversi and Scrocco, reference 1.

TABLE III. Results of the α and α_+ calculated effects.

	1st series (α)		2nd series (α)		3rd series (α_+)	
$\tau/\mu c^2$	$k=0$	$k=\frac{1}{4}$	$k=0$	$k=\frac{1}{4}$	$k=0$	$k=\frac{1}{4}$
1	38.7	17.9	44.8	24.4	56.0	36.2
2	79.5	41.8	78.8	38.6	119.0	66.8
3	100.0	51.1	93.8	47.5	152.1	81.5
4	111.7	55.6	102.6	51.3	171.1	92.5

sponding to the four possible arrangements, *cc*, *dd*, *cd*, *dc* ("convergent" "divergent" referring of course to particles of the specified sign). We may indicate these functions by f_{cc}, f_{dd}, $\cdots$ respectively; if they are known, we may proceed to a theoretical evaluation of (1), (3), and (4).

How these functions can be determined has been discussed elsewhere.[17,18] We shall only recall some results.

We shall put

$$\bar{\sigma}=\sigma-\gamma, \tag{12}$$

which is the value of the "energy" σ possessed by a particle when it reaches the central counter, that is after suffering one-half of the total energy loss in crossing the iron cores. The theory then shows that one has, with sufficient approximation

$$f_{cc}(\sigma,\gamma)=f_{cc}(\bar{\sigma},0);\quad f_{dd}(\sigma,\gamma)=f_{dd}(\bar{\sigma},0);$$
$$\tfrac{1}{2}[f_{cd}(\sigma,\gamma)+f_{dc}(\sigma,\gamma)]=f_{cd}(\bar{\sigma},0)=f_{dc}(\bar{\sigma},0). \tag{13}$$

These formulae have a rather simple meaning; the first two mean, for instance, that the characteristic function can be evaluated by neglecting the energy loss (that is putting $\gamma=0$ in $f(\sigma,\gamma)$) provided the energy $\bar{\sigma}$ instead of the initial energy σ is taken. Then $f(\sigma,\gamma)$ may be indicated more briefly with $f(\bar{\sigma})$. We have found

$$f_{cc}(\bar{\sigma})=1+(1/\bar{\sigma})-(k/\bar{\sigma}^2);$$
$$f_{dd}(\bar{\sigma})=\begin{cases}1-(1/\bar{\sigma})+(1/4\bar{\sigma}^2); & (\bar{\sigma}>\frac{1}{2})\\ 0; & [\bar{\sigma}<\frac{1}{2};\ B>\sim 4.10^3\ \text{gauss}]\end{cases};$$
$$f_{cd}(\bar{\sigma})=f_{dc}(\bar{\sigma})=1+\frac{1+\bar{\sigma}}{2\bar{\sigma}^2}\xi_m^2-\frac{1}{4\bar{\sigma}^2}(3\xi_m+1),$$

where ξ_m is amongst the three real roots of

$$\xi_m^3-2(1+\sigma)\xi_m-1=0,$$

the one which satisfies $-1<\xi_m<0$.

The value of the coefficient k must still be considered. The term containing k has been introduced to take into account in a rough way the effect of scattering within the iron cores, which could not be included in the theory. It is natural to assume that this effect will be important especially at the low energies and especially in the "*cc*" case when the cross section of the counter system tends to increase to very large values with decreasing energy. In our simplified theory this increase continues until the cross section is suddenly brought down to zero, because the particles are stopped in the iron before reaching the lowest counter. Scattering, however, must set a limit to this increase before the stopping limit is reached, and this effect may be represented by a term of the type considered. The choice of the value of k has no considerable influence on the evaluation of the positive excess (see Section 5(a)); unfortunately this is not so in the case of the meson spectrum. We have avoided the difficulty by the assumption that the proper value of k can be determined by comparing our experimental results in air and at sea level with calculations based on formulae (11) and assuming as energy spectrum one that can be derived from the absorption curve in lead measured by Clay and van Gemert. For further details see one of our previous papers;[18] the result is: $k=0.13\pm0.01$.

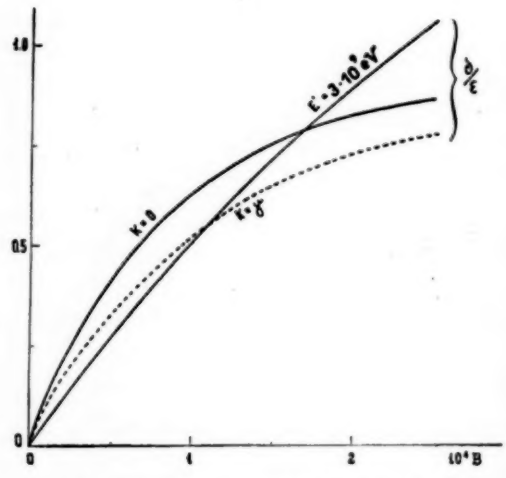

FIG. 7. Theoretical $\delta(B)$ curves (see formula (1)) under the assumptions of a uniformly distributed positive excess (curves $k=0$ and $k=\gamma$) and of an excess localized about $E'=3\times10^9$ ev.

5. DISCUSSION

(a) The Positive Excess

Remembering the definition of N_{ee}, N_{dd}, by means of Eq. (11) we have

$$N_{ee+}=\int_{\gamma}^{\infty}\{\Phi^{+}(\sigma)f_{ee}(\sigma)+\Phi^{-}(\sigma)f_{dd}(\sigma)\}d\sigma,$$
$$N_{dd+}=\int_{\gamma}^{\infty}\{\Phi^{-}(\sigma)f_{ee}(\sigma)+\Phi^{+}(\sigma)f_{dd}(\sigma)\}d\sigma, \tag{14}$$

the meaning of the symbols being self-evident. Assume the positive excess ϵ to be distributed uniformly over the spectrum

$$\Phi^{+}(\sigma)=\tfrac{1}{2}\left(1+\frac{\epsilon}{2}\right)\Phi(\sigma);$$
$$\Phi^{-}(\sigma)=\tfrac{1}{2}\left(1-\frac{\epsilon}{2}\right)\Phi(\sigma). \tag{15}$$

Using the third of Eqs. (10), with $n=3$, we have calculated N_{ee}, N_{dd} as functions of B. From these we derive the $\delta(B)$ curve represented in Fig. 7,[19] which is in good agreement with the approximately linear increase of the experimental δ (Figs. 5, 6). We have found experimentally $\delta=0.15$ for $B=17{,}000$ gauss; comparing this with the two curves of Fig. 7, we find $\epsilon=0.19$ or 0.23 according as we make for k the two extreme assumptions $k=0$, and $k=\gamma$. The exact value of k is therefore rather unimportant, and we may conclude that $\epsilon=20$ percent approximately in very good agreement with Hughes and Jones.

The agreement between the result of Hughes and Jones and our own gives a plausible argument in favor of B as the effective field inside iron.

Subsequently we have also examined different hypotheses about the distribution of the positive excess over the spectrum, but we have found that the shape of the δ *vs.* B curve is rather insensitive to such changes, so that closer investigation of the shape of this curve does not open the possibility of investigating the distribution of the positive excess over the spectrum. The only thing we can say is, that if the excess were located in the low energy part of the spectrum, say around $E<\sim 10^{9}$ ev the value of δ to be expected (for a positive excess of 20 percent) would be considerably larger than observed.

[19] We have not included in the figure the N_{ee} *vs.* B and N_{dd} *vs.* B curves, as derived theoretically; but they also are in good accord with the data of Table I.

TABLE IV. Results of the comparison of theoretical curves for $\alpha(\tau/\mu c^2)$ and experimental results.

Series	$10^{9}\tau/\mu c^{2}$
1st	$2.15\begin{cases}+0.40\\-0.28\end{cases}$
2nd	$2.25\begin{cases}+0.55\\-0.38\end{cases}$
3rd	$2.10\begin{cases}+0.52\\-0.32\end{cases}$

(b) Energy Spectrum

In this case, we assume, for greater accuracy, the meson spectrum to be given by the product of (9) by the probability $W(E, h)$ for a meson of energy E to reach the depth h without disintegrating. In this way the effects α and α_{+}, defined by (3) and (4) are seen to depend on the $\tau/\mu c^2$ ratio, which appears in the expression for $W(E, h)$. If j is the stopping power of air, we shall have $m=hj$. Further we have chosen $n=2.87$ as the most accurate value known to us.[20] For $W(E, h)$ the usual expression was used, and by means of (7) the spectrum was expressed as a function of the dimensionless energy σ.

Assume the positive excess to be uniformly distributed over the spectrum. Writing the explicit expressions of N_{ed} and N_{de} (analogous to (20)) and putting for shortness sake:

$$F(\sigma)=\tfrac{1}{2}[f_{ee}(\sigma)+f_{dd}(\sigma)];$$
$$g(\sigma)=\tfrac{1}{2}[f_{ee}-f_{dd}+f_{ed}-f_{de}],$$

we shall have (see Eq. (2)),

$$N_{ee}=\int_{\gamma}^{\infty}\Phi(\sigma)F(\sigma)d\sigma;$$
$$N_{ed}=\int_{\gamma}^{\infty}\Phi(\sigma)f_{ed}(\sigma)d\sigma \tag{16}$$

while (4) can be expressed approximately[21] in

[20] A. Emhert, Zeits. f. Physik **106**, 751 (1937).

[21] That is neglecting a term $\frac{\epsilon}{4}\int_{\gamma}^{\infty}[f_{de}(\sigma,\gamma)-f_{ed}(\sigma,\gamma)]d\sigma$ compared to N_{ed}.

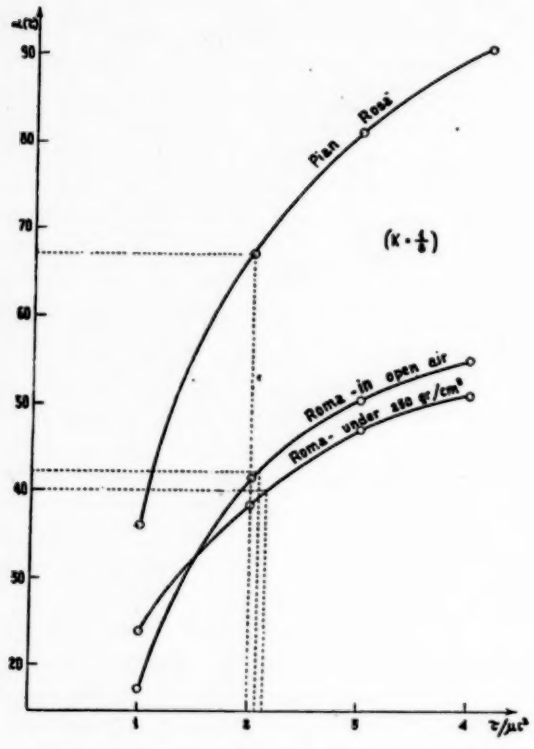

FIG. 8. Comparison of theoretical $\alpha(\tau/\mu c^2)$ curves (see formulas (2)—(4)) and experimental results.

the form

$$\alpha_+=\alpha+\frac{\epsilon}{2N_{cd}}\int_\gamma^\infty \Phi(\sigma)g(\sigma)d\sigma. \qquad (17)$$

The integrals in (16) and (17) have been evaluated numerically, for each of the three series of measurements, for two values of k ($k=0$ and $k=1/8$) and for four values of the ratio $\tau/\mu c^2$ ($=1$; 2; 3; $4\cdot10^{-8}$ sec./Mev). The results are given in Table III. Comparing the calculated $\alpha(\tau/\mu c^2)$ curves (these can be drawn from the results of Table III also for the k values considered in Section 4, remembering the linear dependence of α on k) with the experimental results of Table II, we obtain for $\tau/\mu c^2$ the values contained in Table IV. The essential hypothesis made is that the meson spectrum at the top of the atmosphere can be represented by the law $E^{-2.87}$.

The calculated curves of Fig. 8 confirm the statements already made in Section 3(b) about the influence on α of an absorber 250 g/cm² thick, if one assumes for $\tau/\mu c^2$ a value as low as that found by Nielsen *et al*;[16] the effect observed experimentally has not the sign to be expected on the assumption of a value as low as that.

The values for $\tau/\mu c^2$ derived from the three series of measurements are in surprising agreement with each other, especially considering the fact that the agreement is not sensitive to a change in the initial spectrum. This seems to be one further reason to exclude a complex nature of the meson component,[22] at least between sea level and 4000 m.

Let us now briefly discuss our results. The evaluation of $\tau/\mu c^2$ was based on formula (11); hence it is subject to errors due to (a) the approximations adopted in the theoretical treatment of the characteristic functions and (b) deviations of the actual energy distribution at the top of the atmosphere from the distribution assumed, formula (9).

As regards the first cause of uncertainty a discussion of the hypotheses involved has been given elsewhere[18] but it is rather hard to estimate accurately the possible error. We feel, however, that to assume that this is the source of the difference between our present results and the value, $\tau/\mu c^2\approx3\times10^{-8}$ sec./Mev, which is indicated by the most recent and reliable measurements by the anomalous absorption method,[23] would be to stretch the limits of error of the calculations more than is probable.

We shall, therefore, examine the second possible cause of discrepancy. Obviously one can interpret the discrepancy by the assumption, that the meson energy spectrum on the low energy side is less rich in particles than corresponds to (9). According to this formula the spectrum is given by the product of (9), with $n=2.87$, by the probability of survival $W(E, h)$. This probability was evaluated on the usual assumption that the creation of mesons takes place at a depth of 100 g/cm² below the top. It is well to remark that the value of $W(E, h)$ at sea level is not very sensitive to changes in the depth of the creation layer. Turning now to formula (9), we notice that it is supported by the work of Blackett, Jones, Hughes, and others, for $n=2.9$ and for $E=$ values comprised between

[22] P. Weisz, Phys. Rev. **59**, 554 (1941).
[23] G. Bernardini, Zeits. f. Physik **120**, 413 (1943).

some 10^9 ev and the maximum energies measurable by the Wilson chamber method. The intensity or depth curves of Ehmert and others indicate that the validity of the formula extends to much higher energies. Since moreover the exact shape of the spectrum above 10^{10} ev is immaterial for the present purpose, we may assume the formula $E^{-2.87}$ to represent the *initial* spectrum correctly for all E-values larger than a certain E^*. Considering that in crossing the atmosphere a meson loses about 2.5×10^9 ev, we shall put $E^*\approx4\times10^9$ ev.

For $E<E^*$ the $E^{-2.87}$ law is not sufficiently supported by any experimental data.

There is even some indication to the contrary, for the energy spectra of Hughes and Jones seem to be less rich on the low energy side than one would expect assuming a creation spectrum according to (9), this conclusion being practically unaffected by a variation of the assumed height of the creation layer between 50 and 200 g/cm².

Such a conclusion would be in agreement with our observations and would not lead to any difficulty in connection with present knowledge about the meson radiation in the upper atmosphere. As a matter of fact, the experiments of Schein, Wollan, and Groetzinger,[24] and of Herzog and Bostick,[25] have revealed that a large number of rather slow mesons are created in the upper atmosphere; but these particles are in general much too slow to reach our apparatus and be recorded by it.

One further remark is that the meson spectrum must probably be affected in some way by the cutting off in the spectrum of the primary protons (?) by the magnetic fields of the earth and sun. This would cause a falling off on the low energy side. On the other hand one may compare these suggestions with the results of the measurements of $\tau/\mu c^2$ by the anomalous absorption method based on integral effects. These require hypotheses on the creation spectrum of mesons which are quite analogous to those which are necessary to discuss our experimental results.

As a matter of fact, in the anomalous absorption method, one finds that the agreement between the $\tau/\mu c^2$ values based on differential effects, which are independent of any hypothesis concerning the spectrum, and those based on integral effects, which are not, is in general rather poor. This points to some hypothesis such as we have indicated. Two notable exceptions are given by the measurements discussed by Bernardini and Festa[26] and by the ionization chamber measurements of Neher and Stever.[27] As regards the first exception, however, one may remark that the agreement found may be owing to the evaluation method employed by those authors, a method whose precise aim was to eliminate the uncertainty of the low-energy side of the meson spectrum from the final result.

As regards the experiment of Neher and Stever, one has to remark that it refers to the meson radiation incident from the whole hemisphere; consequently the mean path in air of the particles was much larger than with a vertical counter set. This naturally increases the importance of the high energy side of the spectrum, where no large discrepancies from the $E^{-2.87}$ law need be assumed.

Let us finally turn our attention to the data of the last column in Table II. These allow (see also Section 3(b)) a further evaluation of the positive excess ϵ, on the assumption that it is uniformly distributed over the spectrum. In fact, putting

$$\mu=\frac{1}{N_{ed}}\int_{\gamma}^{\infty}\Phi(\sigma)g(\sigma)d\sigma,$$

we get from (17) and from the analogous expression for α_-

$$\Delta=\mu\epsilon.$$

The evaluation gives:

$$\epsilon=\begin{cases}(18.3\pm4.4)\text{ percent in open air;}\\(18.6\pm5.4)\text{ percent under a layer 250 g/cm}^2\\\quad\text{thick,}\end{cases}$$

in good agreement with the ϵ-value derived from Table I. There is as yet no evidence that the 250 g/cm² layer causes an appreciable change in the positive excess.

We finally wish to emphasize the possibilities

[24] M. Shein, E. O. Wollan, and G. Groetzinger, Phys. Rev. **58**, 1027 (1940).
[25] G. Herzog, and W. H. Bostick, Phys. Rev. **58**, 278 (1940); **59**, 122 (1941).
[26] G. Bernardini and C. Festa, Atti d. R. Acc. D'Italia **7**, 4 (1943).
[27] H. V. Neher and H. G. Stever, Phys. Rev. **58**, 766 (1940).

which the present method may have in the investigation of the meson spectrum at great heights (notice in this connection how the slope of the α *vs.* $\tau/\mu c^2$ curves increases with increasing height). An experiment of this kind by Bernardini and Scrocco was in progress in 1941, but was interrupted by a serious flying accident to the airplane which carried the apparatus. As a consequence the apparatus was gravely damaged, and for this and other reasons connected with Italian events, the experiment was given up for the time being.

PHYSICAL REVIEW VOLUME 68, NUMBERS 5 AND 6 SEPTEMBER 1 AND 15, 1945

Disorder Scattering of X-Rays by Local Distortions

H. EKSTEIN
Armour Research Foundation, Chicago, Illinois
(Received July 16, 1945)

The disorder scattering (background) owing to local distortions is caused mainly by the elastic strain field surrounding the distorted zone rather than by the misfit atoms in the zone of distortion. As an example, the scattering caused by a distortion of spherical symmetry is calculated. The result is extended for more general types of distortions. The background intensity increases strongly in the neighborhood of a line, and it tends toward a constant value for small scattering angles. This explains previous observations on rolled copper.

1

TO explain the plastic properties of solid bodies, it is necessary to assume local lattice distortions or irregularities. Most of the evidence for the assumed models of dislocation is indirect. Several papers have attempted to connect the observed line intensities and widths with the internal distortions.[1–6] Little attention has been given to the continuous background scattering arising from the distortions. The experimental conditions for this type of research are not easy, because other effects such as fluorescent radiation, Compton radiation, diffuse scattering by air, coherent temperature scattering and background owing to the continuous x-ray spectrum, all contribute to the observed background. Yet experiments by Guinier[7] have shown the effect of plastic deformation of copper upon the background to be appreciable. If the scattering caused by local distortions can be isolated, it will provide more useful information than the study of the lines; first, because this scattering is entirely absent in an ideal crystal, while the line intensity decreases only by a few percent when distortion is introduced, and secondly, because slowly variable internal stresses affect the line, but not the background.

The following theoretical discussion gives a correlation between local distortions and disorder scattering, which explains some of Guinier's results, and may be helpful for further experimental work.

For a simple Bravais lattice, the scattering intensity is given by:

$$I = I_e |F|^2 |\sum_n \exp(2\pi i \mathbf{R}\cdot\mathbf{r}_n)|^2, \quad (1)$$

where I_e is the scattering intensity from one electron, F the atomic form factor,

$$\mathbf{R} = \mathbf{k} - \mathbf{k}_0, \quad (2)$$

$\mathbf{k}$ and $\mathbf{k}_0$ the wave vectors of incident and scattered wave, and $\mathbf{r}_n$ the radius vector of the nth atom. For $\mathbf{r}_n$, we write

$$\mathbf{r}_n = \mathbf{a}_n + \mathbf{u}_n, \quad (3)$$

[1] J. Hengstenberg and H. Mark, Zeits. f. Physik **61**, 435 (1930).
[2] G. W. Brindley and F. W. Spiers, Phil. Mag. **20**, 882 (1935).
[3] U. Dehlinger, Zeits. f. Krist. **65**, 615 (1927).
[4] W. Boas, Zeits. f. Krist. **97**, 354 (1937).
[5] U. Dehlinger and A. Kochendörfer, Zeits. f. Metallkunde **31**, 231 (1939).
[6] A. Kochendörfer, Zeits. f. Krist. **101**, 149 (1939).
[7] A. Guinier, Comptes rendus **208**, 894 (1939).

where $\mathbf{a}_n$ is the radius vector of the nth lattice point.

In physical lattice distortions of the type usually assumed, the displacements of the atoms from the regular lattice points are of the order of magnitude of the atomic distances in the immediate neighborhood of the distortion which extends over only a few atomic distances. The number of atoms within this zone is small, and they cannot be expected to give a large contribution to the disorder scattering. Outside the distortion zone itself, the displacement of atoms is of the elastic type, i.e., the displacements are small as compared to the atomic distance. While the displacement decreases rapidly from the origin of the perturbation, the number of atoms affected is large, and we may expect an important x-ray effect from them.

In the following the atoms within the distorted zone in this sense are disregarded, and only the indirect effect of the distortion, through its elastic strain field, is taken into account.

Consequently, we may assume that in Eq. (3) $\mathbf{u}_n$ is small in comparison to the interatomic distance. With the notation

$$G=\sum_n \exp(2\pi i\mathbf{R}\cdot\mathbf{r}_n), \tag{4}$$

the Taylor expansion yields:

$$G=\sum_n \exp(2\pi i\mathbf{R}\cdot\mathbf{a}_n) + 2\pi i\mathbf{R}\cdot\left(\sum_n \mathbf{u}_n \exp(2\pi i\mathbf{R}\cdot\mathbf{a}_n)\right) + \cdots = G_0+G_1\cdots \tag{5}$$

The first term of (5) represents the ordinary scattering by a regular crystal and can be disregarded here. As we are interested only in the scattering outside the lines, the second term may be treated separately.

In order to bring the second term of (5) into a more convenient form, we use a transformation formula given by Ewald.[8] If $\mathbf{A}_h$ are the lattice vectors of the reciprocal lattice and v the volume of the unit cell, then

$$\sum_n u_n \exp(2\pi i\mathbf{R}\cdot\mathbf{a}_n)=\frac{1}{v}\sum_h U(\mathbf{R}-\mathbf{A}_h), \tag{6}$$

where $U(\mathbf{R})$ is the Fourier transform of a function $u(\mathbf{r})$ which interpolates the values u_n at the lattice points:

$$U(\mathbf{R})=\int u(\mathbf{r}) \exp(2\pi i\mathbf{R}\cdot\mathbf{r})dv, \tag{7}$$

and

$$u(\mathbf{r}=\mathbf{a}_n)=u_n. \tag{8}$$

This transformation may be considered as a three-dimensional generalization of Poisson's sum formula. Patterson's representation of the interference function of perfect crystals[9] can be recognized as a special application of the generalized Poisson formula.

The Eqs. (6)–(8) are evidently still applicable if the quantities u_n are vectors, $\mathbf{u}_n$, if only the functions $u(\mathbf{r})$ and $U(\mathbf{R})$ are replaced by vector functions $\mathbf{u}(\mathbf{r})$ and $\mathbf{U}(\mathbf{R})$. Equations (6)–(8) become:

$$\sum_n \mathbf{u}_n \exp(2\pi i\mathbf{R}\cdot\mathbf{a}_n)=\frac{1}{v}\sum_h \mathbf{U}(\mathbf{R}-\mathbf{A}_h), \tag{6a}$$

$$\mathbf{U}(\mathbf{R})=\int \mathbf{u}(\mathbf{r}) \exp(2\pi i\mathbf{R}\cdot\mathbf{r})dv, \tag{7a}$$

$$\mathbf{u}(\mathbf{r}=\mathbf{a}_n)=\mathbf{u}_n. \tag{8a}$$

The Eqs. (7) and (8) do not determine uniquely the function $\mathbf{U}$ because any function which interpolates the values $\mathbf{u}_n$ is acceptable for $\mathbf{u}(\mathbf{r})$.

The disorder scattering function G_1 is built up of a number of identical functions having their respective origins at lattice points of the reciprocal lattice. The advantage of this transformation is that the function $\mathbf{U}(\mathbf{R})$ often decreases so rapidly from $\mathbf{R}=0$, that near a lattice point $\mathbf{A}_i$ of the reciprocal lattice, all terms of the sum (6) can be neglected except the term $\mathbf{U}(\mathbf{R}-\mathbf{A}_i)$.

2

As an example, the case of spherical dilatation will be considered. If one or several atoms are inserted into the lattice in addition to the regular atoms or if a larger atom is substituted for a regular one, then the neighboring atoms will be pushed radially outwards. In most metal crystals each atom is surrounded by a sizable number of equidistant atoms so that it is reasonable to replace the central perturbation by a spherical cavity with a pressure p_1. Furthermore, the resultant displacements will be calculated as if

[8] P. P. Ewald, Göttinger Nachrichten 55 (1938).

[9] A. L. Patterson, Phys. Rev. 56, 972 (1939).

the crystal were isotropic, because the results will be interesting mainly for their order of magnitude. According to Love,[10] the radial displacement u in a shell bounded by concentric spherical surfaces of radii r_0 and $r_1(r_0>r_1)$ is given by

$$u=\frac{1}{3\lambda+2\mu}\frac{p_1r_1^3}{r_0^3-r_1^3}\cdot r+\frac{1}{4\mu}\frac{r_0^3r_1^3p_1}{r_0^3-r_1^3}\cdot\frac{1}{r^2}. \quad (9)$$

In our case the crystal size r_0 is large as compared to the radius of the distortion r_1 so that the first term in Eq. (9) can be neglected. Similarly, we disregard the term r_1^3 in the denominator of the second term of (9). The displacement u_1 at the inner surface is

$$u_1=(r_1/4\mu)p_1, \quad (10)$$

and we get instead of (9)

$$u=u_1(r_1^2/r^2). \quad (11)$$

Inserting (11) into (7a), we obtain

$$\mathbf{U}=u_1r_1^2\int\frac{\mathbf{r}}{r^3}\exp(2\pi i\mathbf{R}\cdot\mathbf{r})dv. \quad (12)$$

Because of the spherical symmetry of the displacement, $\mathbf{U}$ must be parallel to $\mathbf{R}$:

$$U_R=u_1r_1^2\int\frac{\cos(\mathbf{r},\mathbf{R})}{r^2}\exp(2\pi i\mathbf{R}\cdot\mathbf{r})dv,$$
$$=\frac{2iu_1r_1^2}{R}\left(\frac{\sin 2\pi r_1R}{2\pi r_1R}-\frac{\sin 2\pi r_0R}{2\pi r_0R}\right). \quad (13)$$

This function vanishes at $R=0$, but beyond a maximum at $R=1/2r_0$, the first term rapidly becomes predominant. Now, the central spot of the interference function G_0 which gives rise to the x-ray line itself, extends to about $R=2/r_0$. As the disorder scattering cannot be measured in the immediate neighborhood of the line, we may limit ourselves to such points which are well outside the line. In the following, this domain will be called "near the lattice point" (of the reciprocal lattice) or, "near the line." With this restriction, U_R becomes

$$U_R=iu_1r_1\frac{\sin 2\pi r_1R}{\pi R^2}, \quad (14)$$

and, by Eqs. (6a) and (5)

$$G_1=\frac{-2u_1r_1}{v}R\sum_h\cos(\mathbf{R},\mathbf{R}-\mathbf{A}_h)\times\frac{\sin 2\pi r_1|\mathbf{R}-\mathbf{A}_h|}{|\mathbf{R}-\mathbf{A}_h|^2}. \quad (15)$$

Now, the distance between two neighboring lattice points of the reciprocal lattice is of the order of the inverse interatomic distance. As r_1 is of the order of this latter quantity, it may be seen from (14) and (5) that the bulk of the function which constitutes the contribution of a particular lattice point $\mathbf{A}_i$ will be contained in the space between $\mathbf{A}_i$ and its immediate neighbors. Near any lattice point, we may disregard the contributions of all other lattice points, because of the rapid increase of the individual function $\mathbf{U}(\mathbf{R}-\mathbf{A}_i)$.

The surrounding of the lattice point (000), i.e., of the direct transmitted beam, assumes a special place. By Eq. (5), the disorder scattering is proportional to R, and furthermore $\sum\mathbf{u}_n$ vanishes because the center of gravity is at rest, so that we should expect the disorder scattering to tend toward zero near the direct beam. The physical significance of this fact was explained by Ewald[11] by the observation that even an asphalt road makes a fairly good mirror when observed at a very oblique angle. Yet, according to Eq. (15), the predominant term of the sum is that which corresponds to $\mathbf{A}_h=0$; $\mathbf{R}$ becomes equal to $(\mathbf{R}-\mathbf{A}_h)$:

$$G_1\cong-\frac{2u_1r_1}{v}\frac{\sin 2\pi r_1R}{R}, \quad (16)$$

and G_1 tends toward a constant value at $R=0$. This is true, as explained above, only for points not too close to the line (000) itself, but it describes the experimental form of the disorder scattering curve. Indeed, Guinier's experiments show that the background intensity of cold worked copper becomes constant near the scattering angle zero. As the Compton radiation as well as the temperature scattering tends toward zero at small angles, it is probable that the effect is caused by a perturbation similar to that considered here.

[10] A. E. H. Love, *Mathematical Theory of Elasticity* (Cambridge University Press, New York, 1934), p. 142.

[11] P. P. Ewald, *Handbuch der Physik* (Berlin, 1927), Vol. 24, p. 271.

Equation (14) predicts a strong increase of intensity near a reciprocal lattice point. This, too, is in agreement with Guinier's observations. The exact form of the intensity curve for a polycrystalline aggregate would be given by the average of $|G_1|^2$ over all crystal orientations, the absolute value $|\mathbf{R}|$ being fixed for a given scattering angle. But this integration would not have a result comparable to Guinier's experiments. Indeed, G_1 is proportional to the cosine of the angle between $\mathbf{R}$ and $(\mathbf{R}-\mathbf{A}_h)$ in the example under consideration, and this is owing to the spherical symmetry of the perturbation assumed in this section. We cannot expect the local perturbation created by plastic deformation to have a spherical symmetry, so that our example would not be typical for the general case.

3

The results of the preceding section are susceptible of considerable generalization. In this section, an infinitely extended body with a local perturbation of general character and no forces at infinity will be considered. The action of the local distortion will be replaced by a system of volume forces $\mathbf{f}(\mathbf{r})$, confined within a volume of atomic order of magnitude. The resultant force,

$$\int \mathbf{f}(\mathbf{r})dv,$$

must vanish if there are no boundary stresses. The laws of isotropic elasticity will again be used.

This method differs from that of Section 2, where the distorted zone was replaced by a cavity, in that the atomic configuration within the distorted zone is replaced by one which is formally in agreement with elastic equilibrium and the fictitious volume force. However, because of the small number of these atoms, no appreciable difference between the two methods should arise.

If the displacement $\mathbf{u}(\mathbf{r})$ is represented by a Fourier integral

$$\mathbf{u}(\mathbf{r}) = \int \mathbf{U}(\mathbf{R}) \exp(-2\pi i \mathbf{R}\cdot\mathbf{r})dV, \quad (17)$$

then the inversion of Eq. (17) is Eq. (6a). By differentiating under the integral sign, we obtain from Eq. (17):

$$\Delta\mathbf{u} = -4\pi^2 \int R^2\mathbf{U} \exp(-2\pi i \mathbf{R}\cdot\mathbf{r})dV, \quad (18)$$

grad div $\mathbf{u}$

$$= -4\pi^2 \int \mathbf{R}\cdot(\mathbf{R}\cdot\mathbf{U}) \exp(-2\pi i \mathbf{R}\cdot\mathbf{r})dV. \quad (19)$$

The force function $\mathbf{f}(\mathbf{r})$ will also be represented by a Fourier integral:

$$\mathbf{f}(\mathbf{r}) = \int \mathbf{F}(\mathbf{R}) \exp(2\pi i \mathbf{R}\cdot\mathbf{r})dV, \quad (20)$$

with the inversion:

$$\mathbf{F}(\mathbf{R}) = \int \mathbf{f}(\mathbf{r}) \exp(-2\pi i \mathbf{R}\cdot\mathbf{r})dv. \quad (21)$$

The equation of elastic equilibrium:

$$\mu\Delta\mathbf{u} + (\lambda+\mu) \text{ grad div } \mathbf{u} + \rho\mathbf{f} = 0, \quad (22)$$

becomes, by Eqs. (18)–(20):

$$\int \exp(-2\pi i \mathbf{R}\cdot\mathbf{r})$$

$$\times[-4\pi^2\mu R^2\mathbf{U} - 4\pi^2\mathbf{R}\cdot(\mathbf{R}\cdot\mathbf{U}) + \rho\mathbf{F}]dV = 0. \quad (23)$$

By virtue of a general theorem, the transform must vanish:

$$\mu R^2\mathbf{U} + (\lambda+\mu)\mathbf{R}\cdot(\mathbf{R}\cdot\mathbf{U}) = \frac{\rho}{4\pi^2}\mathbf{F}. \quad (24)$$

The solution of this vector equation is:

$$\mathbf{U} = \frac{\rho}{4\pi^2 R^4}\left(\frac{\mathbf{R}\times(\mathbf{F}\times\mathbf{R})}{\mu} + \frac{\mathbf{R}\cdot(\mathbf{F}\cdot\mathbf{R})}{\lambda+2\mu}\right). \quad (25)$$

We are interested in the behavior of $\mathbf{U}$ at small values of $|\mathbf{R}|$. Expansion of Eq. (21) yields:

$$\mathbf{F} = \int \mathbf{f}dv + 2\pi i \int (\mathbf{R}\cdot\mathbf{r})\mathbf{f}dv + \cdots. \quad (26)$$

The first term is the resultant force, and therefore, vanishes. Introducing the expansion (26) into Eq. (25), it can be seen that $\mathbf{U}$ behaves like $1/R$ for small values of R.

This is the generalization of the result of Section 2. In particular, it can be seen from

Eqs. (5) and (6a) that near the lattice point (000), the scattering amplitude and consequently the intensity tend toward a constant value, in agreement with Guinier's observations.

The results of this section are valid only for infinitely extended crystal grains. When the grain is finite, but large enough to give rise to sharp lines, the statements of this section remain valid only for points well outside the line, as was shown in Section 2.

Near a lattice point $\mathbf{A}_h$, the scattering amplitude will be given by

$$G_1=\frac{2\pi i}{v}|\mathbf{A}_h|\cos(\mathbf{A}_h,\mathbf{U})\cdot|\mathbf{U}(\mathbf{R}-\mathbf{A}_h)|. \quad (27)$$

Now, if the force system $\mathbf{f}$ has a privileged crystallographic direction, then we must expect to obtain different scattering near different lattice points of similar absolute distance $|\mathbf{A}_h|$, because of the direction cosine appearing in Eq. (27). Conversely, observations of the disorder scattering near different lines should be able to show the crystallographic symmetry of distortions.

A disorder scattering of the type under consideration must affect the measured line intensity and line width. However, conditions are more complex within the line itself, because the grain size and the slowly variable stresses account for part of the line broadening.[6]

PHYSICAL REVIEW VOLUME 68, NUMBERS 5 AND 6 SEPTEMBER 1 AND 15, 1945

Special Cases of Predissociation

B. ROSEN
Department of Astrophysics, University of Liége, Liége, Belgium
(Received July 27, 1945)

A study of the AlO spectrum indicates that a predissociation of the type one b takes place in the lower electronic state of the green system. It is suggested that the γ- and ϵ-bands of NO do not belong to a single system; the γ system shows a strong perturbation of the $v'=4$ level. An accidental predissociation of the vibrational type is found in the spectrum of Te_2, and the analogy of the three molecules S_2, Se_2, and Te_2 is strengthened.

AlO

ONLY a few examples of predissociation involving the lower state of a molecule are known, among which the best studied case is that of HgH. However, in the type III of predissociation (by rotation) exhibited by HgH the widening of the predissociated levels is such that they cannot be observed. Holst[1] has reported predissociation effects in two systems of emission bands of AlH due to transitions ending on the unstable $^1\Pi$ level. But, so far as we know, this example has not been studied in detail. The observation of the predissociated lines in the above-mentioned examples is difficult on high dispersion spectrograms, on account of the intensity drop in the centers of the lines.

It is well known that, as a result of the rise in total absorption in the incompletely resolved predissociated lines (Loomis and Fuller),[2] predissociation may, under certain conditions be observed in absorption even with low dispersion. This criterion has been applied previously to the investigation of induced predissociation. In the case of natural predissociation, the criterion was first applied to the H_2 spectrum by Beutler, Deubner, and Jünger,[3] and to the S_2 spectrum by Rosen and Neven.[4] The latter example has recently been investigated in detail by Herzberg and Mundie.[5]

In emission, the widening of the lines of incompletely resolved bands manifests itself in different manners according to the position of

[1] W. Holst, Thesis (Trondheim, 1936).

[2] F. Loomis and H. Fuller, Phys. Rev. **39**, 180 (1932).
[3] H. Beutler, A. Deubner, and H. O. Jünger, Zeits. f. Physik **98**, 181 (1935).
[4] B. Rosen and L. Neven, Comptes rendus **203**, 662 (1936); J. Chim. Phys. **35**, 58 (1938).
[5] G. Herzberg and L. C. Mundie, Phys. Rev. **8**, 263 (1940).

the first predissociated line relative to the head. If this first predissociated line is far removed from the head, a sudden breakdown in intensity should be observed, the band being thus shorter than the non-predissociated ones. If the predissociation occurs at a J-value nearer to the head, the effect of intensity drop may be partly compensated by the superposition of widened neighboring lines. Finally, a predissociation occurring in the region of the head should result in an abnormal weakening of the whole band, which should then appear diffuse and degraded in both directions. As the J-value corresponding to the head varies from one band to another, the extension and intensity of the bands in a given v'' progression varies in a characteristic manner according to v'. We have observed these characteristic changes in the spectrum of AlO and have applied them to the study of predissociation. In the $v''=7$ progression, for instance, the following observations can be made. The (4, 7) band is abnormally weak; it is diffuse and degraded in both directions. The (5, 7) band has a normal intensity in the region of the head, but this band is short and slightly degraded to the violet in addition to the normal degradation to the red. The (6, 7) and following bands have normal intensities and become gradually longer, the breakdown of intensity occurring at a greater distance from the head. Owing to superpositions, an accurate determination of the position of the breakdown is possible for the (9, 7) and (10, 7) bands only; it occurs in the former at a distance of 28 cm^{-1} from the head, in the latter at a distance of 37 cm^{-1}. From the molecular constants of the green system of AlO it is found that the intensity drop corresponds to $K=44$, $v''=7$. In the same manner the observations in the $v''=6$ progression are explained by a predissociation at $K=60$, and those in the $v''=8$ progression by a predissociation at $K=8$, whereas all the bands of the $v''=9$ progression seem to be predissociated.

The application of Herzberg's theory to these results indicates that the predissociation takes place in the lower state of the $^2\Sigma-{}^2\Sigma$ system of AlO, that it belongs to the type one b, and that the asymptote of the perturbing state is situated 0.93 volt above the $v''=0$, $K=0$ state of the lower $^2\Sigma$ level. It is probable that the predissociation observed by Coheur-Dehalu[6] in the (0, 0) band at $K=128$ belongs to the same limiting curve of predissociation.

The lower state of the $^2\Sigma$ system is generally considered as being the normal state of AlO, this system being observed in absorption in the laboratory under special conditions. On the other hand the vibrational levels of this state are known up to 2.2 ev.[7] It follows that one of the atoms resulting from the dissociation of AlO in the normal state must be excited; probably the end products of the dissociation are $Al(^2P)$ and $O(^1D)$. A detailed account will be published elsewhere.

NO

Herzberg and Mundie[8] have suggested that the bands previously attributed to the γ- and ϵ-systems of NO belong to a single system, the ϵ-bands corresponding to transitions to the levels $v\geq 4$ of the $^2\Sigma$ state. The considerably greater intensity of the ϵ-bands is explained as a predissociation effect.

The observation by Guillery[8] of γ-emission bands corresponding to $v\geq 4$ was not considered by Herzberg and Mundie as a conclusive objection to their suggestion. But Guillery's observation, together with several other facts, such as the general character of the absorption bands of NO studied by Leifson[9] made a re-examination of this question desirable. Measures by P. Migeotte and the writer of all the NO bands excited in emission have enabled us to improve the vibrational classification of the γ-bands previously published by Guillery on the basis of the measures by Bair and Deslandres. A considerable perturbation of the vibrational type (displacement of about 90 cm^{-1}) affects the $v'=4$ level, but the γ-bands attributed by Guillery to $v'\geq 4$ appear with great intensity. An elaborate discussion to be published soon proves conclusively that these bands belong to the γ-system. In addition, our observations of the emission bands in the region of 1900A exclude the possibility of considering the ϵ-bands as part of

[6] F. Coheur-Dehalu, Bull. Acad. Roy. Belgium **23**, 604 (1937).
[7] E. Bodson and F. Coheur-Dehalu, Bull. Acad. Roy. Belgium **23**, 408 (1937).
[8] M. Guillery, Zeits. f. Physik **42**, 121 (1927).
[9] S. W. Leifson, Astrophys. J. **63**, 73 (1926).

the γ-system. Hence the hypothesis of Herzberg and Mundie and its conclusions should be abandoned.[10]

Te_2

In collaboration with R. Migeotte we have recently studied the ultraviolet part of the Te_2 spectrum.[11] The following observation concerning a predissociation effect is of interest. The ultraviolet end of the Te_2 spectrum consists of the $v''=0$ progression. Theoretically this progression should have a regular intensity distribution with a single maximum. This is what we observe in absorption, the maximum being found at $v'=15$. In emission, however, the bands $v'=14$ and $v'=16$ are abnormally weak (for the numbering of the Te_2 bands).[12] It seems that we are confronted with a predissociation phenomenon which can be accounted for as an accidental predissociation of the vibrational type analogous to a vibrational perturbation affecting a whole band.

The unresolved isotopic bands $v'=14$ and $v'=16$ are not only weakened, but they present in emission a very pronounced asymmetry. In connection with the observations of Olsson,[13] who states that the positions of the individual absorption bands are quite normal, this means that the weakening by accidental predissociation is different for different individual isotopic bands. No such asymmetry is observed in absorption.

Two regions of predissociation are known in the S_2 and Se_2 spectra. In S_2, predissociation occurs at the levels $v'\geq 10$ and $v'\geq 17$[5] whereas in Se_2 it occurs at the levels $v'\geq 10$ and $v'\geq 22$.[14] In the spectrum of Te_2 only one predissociation region, setting in at $v'=21$, has been reported.[15] Our new observation indicates that the Te_2 molecule also can predissociate at intermediate v' values. However, contrary to the other molecules of the same group, the predissociation of Te_2 at intermediate v' values is only possible through an intermediate state, by an accidental predissociation of the vibrational type. The close analogy existing between the spectra of the three molecules is thus strengthened, especially since considerable perturbations of the vibrational type are known for numerous excited levels of S_2 and Se_2.

[10] We have recently published a detailed investigation of the various ultraviolet band systems of NO (Bull. Soc. Roy. Sci., Liége, Belgium, pp. 40 and 49, 1945). Subsequently we have learned that three papers had been recently published on the NO molecule, one by Gerö, Schmid, and Szily (Physica **9**, 144 (1944)); the others by Gaydon (Proc. Phys. Soc. **56**, 95, and 160 (1944)). As far as predissociation is concerned, these authors reach the same conclusion as we do.

[11] R. Migeotte and B. Rosen, Bull. Soc. Roy. Sci., Liége (in press).

[12] R. Migeotte, Bull. Soc. Roy. Sci., Liége **13**, 48 (1942).

[13] E. Olsson, Thesis (Stockholm, 1938); Zeits. f. Physik **95**, 215 (1935).

[14] B. Rosen, Physica **6**, 205 (1939).

[15] E. Hirschlaff, Zeits. f. Physik **75**, 315 (1932).

PHYSICAL REVIEW VOLUME 68, NUMBERS 5 AND 6 SEPTEMBER 1 AND 15, 1945

Space Charge between Coaxial Cylinders

LEIGH PAGE AND NORMAN I. ADAMS, JR.
Sloane Physics Laboratory, Yale University, New Haven, Connecticut

(Received August 12, 1945)

New solutions of the space charge equation are obtained, which converge much more rapidly than Langmuir's solution in the important case where the radius of the outer electrode is large compared with that of the inner electrode.

THE theory of the limitation of a current by space charge in an evacuated region containing ions of one sign only was given first by Child[1] for parallel plane electrodes and later by Langmuir[2] and Langmuir and Blodgett[3] for the far more important case of coaxial cylindrical electrodes, as found in the usual construction of

[1] C. D. Child, Phys. Rev. **32**, 498 (1911).

[2] I. Langmuir, Phys. Rev. **2**, 450 (1913).

[3] I. Langmuir and K. B. Blodgett, Phys. Rev. **22**, 347 (1923).

the diode vacuum tube. In the first case the solution is obtained easily in closed form, but in the second a non-linear differential equation is encountered which can be solved only in series. Langmuir's solution is a power series in the logarithm of the ratio of the distance r from the common axis of the electrodes to the radius a of the inner electrode or cathode. While this series converges satisfactorily for small values of r/a, it converges very poorly in the much more important region where r/a is large, and special approximate methods had to be employed for values of r/a greater than 66. The object of the present paper is to develop a solution which converges the better the larger is the ratio r/a. In fact, five terms of the solution obtained give an accuracy of two or three parts in ten thousand for all values of r/a greater than 3.

If e/m is the ratio of charge to mass of the ions (electrons) in the tube, $V(r)$ the excess of the potential over that of the cathode, $\rho(r)$ the charge density, and j_l the current per unit legnth of the coaxial electrodes, the equations to be satisfied are, in Heaviside-Lorentz units,

$$\dot{r}^2 = -\frac{2e}{m}V, \tag{1}$$

$$\frac{1}{r}\frac{d}{dr}\left(r\frac{dV}{dr}\right) = -\rho, \tag{2}$$

$$j_l = 2\pi\rho r\dot{r}, \tag{3}$$

subject to the boundary conditions

$$dV/dr = 0, \quad \rho = \infty, \tag{4}$$

at $r=a$. The boundary conditions imply saturation current and negligible initial velocities.

Eliminating ρ and $\dot{r}$, we find, if we put $\eta \equiv a/r$,

$$j_l = \frac{8\pi}{9}\left(\frac{2e}{m}\right)^{\frac{1}{2}}\frac{(-V)^{\frac{1}{2}}}{rg(\eta)}, \tag{5}$$

where $g(\eta)$ satisfies the non-linear differential equation

$$g\left[3\eta\frac{d}{d\eta}\left(\eta\frac{dg}{d\eta}\right) - 4\eta\frac{dg}{d\eta} + 2(g-1)\right] = \left[\eta\frac{dg}{d\eta}\right]^2, \quad 0 \leqslant \eta \leqslant 1. \tag{6}$$

The function g is identical[4] with Langmuir's β^2.

It is obvious that $g=1$ satisfies (6). Hence to obtain a solution which converges rapidly for large r or small η, it would be natural to try the power series

$$g = 1 + a_1\eta + a_2\eta^2 + \cdots.$$

However, substitution in the differential equation shows that a power series solution in η does not exist. Hence we change the independent variable from η to z, getting in place of (6)

$$g\left[3\eta^2\left(\frac{dz}{d\eta}\right)^2\frac{d^2g}{dz^2} + 3\eta^2\frac{d^2z}{d\eta^2}\frac{dg}{dz} - \eta\frac{dz}{d\eta}\frac{dg}{dz} + 2(g-1)\right] = \left[\eta\frac{dz}{d\eta}\frac{dg}{dz}\right]^2,$$

and assume a power series solution in z, to wit:

$$g = 1 + a_1 z + a_2 z^2 + \cdots.$$

Substituting in the differential equation and equating the coefficients of a_1 on both sides, we find that a_1 is arbitrary provided

$$3\eta^2\frac{d^2z}{d\eta^2} - \eta\frac{dz}{d\eta} + 2z = 0,$$

the solution of which is

$$z = A_1\eta^{p_1} + A_2\eta^{p_2},$$

where

$$p_1 \equiv \frac{2+i(2)^{\frac{1}{2}}}{3}, \quad p_2 \equiv \frac{2-i(2)^{\frac{1}{2}}}{3}.$$

Now put

$$y \equiv \eta^{\frac{1}{2}}, \quad \beta \equiv \frac{(2)^{\frac{1}{2}}}{2}\log y + \alpha.$$

Then a power series solution in

$$z_1 \equiv cye^{i\beta}, \quad z_2 \equiv cye^{-i\beta},$$

exists, of the form

$$g = 1 + (z_1+z_2) + (a_{11}z_1^2 + a_{12}z_1z_2 + a_{22}z_2^2) + (a_{111}z_1^3 + a_{112}z_1^2z_2 + a_{122}z_1z_2^2 + a_{222}z_2^3) + \cdots. \tag{7}$$

This is a *complete* solution, since it contains the two arbitrary constants c and α.

[4] The reason for this departure from an established notation is that our treatment leads to a differential equation in g, and it would be awkward and unusual to express the dependent variable as the square of a function.

To evaluate the coefficients in (7), it is convenient to change the independent variable in (6) from η to y. Then

$$g\left[3y\frac{d}{dy}\left(y\frac{dg}{dy}\right)-6y\frac{dg}{dy}+\frac{9}{2}(g-1)\right]=\left[y\frac{dg}{dy}\right]^2, \quad (8)$$

and we find for the first five terms of the solution[5]

$$\begin{aligned}g=1&+2cy\cos\beta\\&+2c^2y^2\left[\frac{5}{33}\cos 2\beta+\frac{2(2)^{\frac{1}{2}}}{33}\sin 2\beta+\frac{1}{3}\right]\\&+2c^3y^3\left[-\frac{17}{594}\cos 3\beta+\frac{19(2)^{\frac{1}{2}}}{2376}\sin 3\beta\right.\\&\left.+\frac{1}{396}\cos\beta+\frac{(2)^{\frac{1}{2}}}{264}\sin\beta\right]\\&+2c^4y^4\left[\frac{2386}{421{,}443}\cos 4\beta\right.\\&-\frac{7541(2)^{\frac{1}{2}}}{1{,}685{,}772}\sin 4\beta-\frac{91}{33{,}858}\cos 2\beta\\&\left.-\frac{82(2)^{\frac{1}{2}}}{16{,}929}\sin 2\beta+\frac{17}{11{,}286}\right]+\cdots. \quad (9)\end{aligned}$$

When we attempt to determine the constants c and α from the boundary conditions $g=0$ and $dg/dy=0$ at $y=1$, we find that this series does not converge rapidly enough for this value of y to ensure the desired accuracy of one part in a thousand from the five terms computed. Instead of calculating further terms we have developed a second series which converges very rapidly in the neighborhood of $y=1$, and then made use of the principle of analytic continuation to fit the series (9) to it. This second series is a power series in $x\equiv 1-y=1-\eta^{2/3}$.

Changing the independent variable in (8) from y to x we have

$$g\left[3(1-x)\frac{d}{dx}\left\{(1-x)\frac{dg}{dx}\right\}+6(1-x)\frac{dg}{dx}+\frac{9}{2}(g-1)\right]=\left[(1-x)\frac{dg}{dx}\right]^2, \quad 0\leqslant x\leqslant 1. \quad (10)$$

[5] After expressing the solution in trigonometrical form, the numerical coefficients were checked by substituting back in the differential equation.

In order to satisfy the boundary conditions at the cathode, the function g must be of the form

$$g=\frac{9}{4}x^2[1+b_1x+b_2x^2+\cdots].$$

We find the following recursion formula for the coefficients:

$$\begin{aligned}(3p+2)(p+1)b_p=&[6p^2-5.6p-2]b_{p-1}\\&-[3p^2-10.756{,}667p+10.41]b_{p-2}\\&+[(5b_3-8b_2+3b_1)p\\&\quad-(65b_3-68b_2+16.5b_1)]b_{p-3}\\&+[(6b_4-10b_3+4b_2)p\\&\quad-(102b_4-125b_3+36.5b_2)]b_{p-4}\\&+[(7b_5-12b_4+5b_3)p\\&\quad-(147b_5-198b_4+64.5b_3)]b_{p-5}\\&+[(8b_6-14b_5+6b_4)p\\&\quad-(200b_6-287b_5+100.5b_4)]b_{p-6}\\&\cdots\cdots\cdots\cdots\\&+[(\cdots)p-(\cdots)]b_1, \quad (11)\end{aligned}$$

where first differences are constant in the coefficient of p and second differences in the other

TABLE I.

r/a	x	g from (12)	y	g from (14)
1	0	0		
2	0.37004	0.2793		
3	0.51925	0.5171	0.48075	0.5170
4	0.60315	0.6671	0.39685	0.6670
5	0.65800	0.7666	0.34200	0.7667
6	0.69715	0.8363	0.30285	0.8363
7	0.72672	0.8870	0.27328	0.8870
8	0.75000	0.9254	0.25000	0.9254
9	0.76888	0.9550	0.23112	0.9549
10			0.21544	0.9782
11			0.20218	0.9970
12			0.19079	1.0123
20			0.13572	1.0716
40			0.08550	1.0947
80			0.05386	1.0846
160			0.03393	1.0634
320			0.02137	1.0422
640			0.01347	1.0253
1280			0.00848	1.0135
2560			0.00534	1.0060
5120			0.00337	1.0019
10240			0.00212	0.9998
20480			0.00134	0.9991
40960			0.00084	0.9990
81920			0.00053	0.9991

term. This gives for the solution

$$g=\frac{9}{4}x^2[1-0.200{,}000x-0.110{,}833x^2$$
$$-0.065{,}303x^3-0.042{,}006x^4$$
$$-0.028{,}876x^5-0.020{,}858x^6$$
$$-0.015{,}647x^7-0.012{,}091x^8$$
$$-0.009{,}568x^9-0.007{,}720x^{10}$$
$$-0.006{,}330x^{11}-0.005{,}261x^{12}$$
$$-0.00442x^{13}-0.00375x^{14}$$
$$-0.00321x^{15}-\cdots]. \quad (12)$$

This series is superior to that given by Langmuir in that the variable goes to unity instead of infinity as r/a increases without limit.

After a few trials it appeared that $x=2/3$, $y=1/3$ was the best point at which to fit the complete solution (9) to the solution (12) satisfying the boundary conditions. At this point

$$g=0.78220, \quad y\frac{dg}{dy}=-0.59784,$$

which gives

$$c=-0.9780, \quad \alpha=-22°.83,$$

to one part in a thousand. Consequently, if we put

$$\theta\equiv 93°.288\log_{10}(1/y)+22°.83 \quad (13)$$

to avoid negative signs, the solution (9) satisfying the specified boundary conditions at the cathode is

$$g=1-[1.9560\cos\theta]y+[0.63767$$
$$+0.28985\cos 2\theta-0.16396\sin 2\theta]y^2$$
$$-[0.00472\cos\theta-0.01002\sin\theta$$
$$-0.05354\cos 3\theta-0.02116\sin 3\theta]y^3$$
$$+[0.00276-0.00492\cos 2\theta$$
$$+0.01253\sin 2\theta+0.01036\cos 4\theta$$
$$+0.01158\sin 4\theta]y^4-\cdots. \quad (14)$$

These five terms give an accuracy of better than one part in a thousand for all r/a greater than three. In fact, for r/a greater than ten the first four terms are sufficient, for r/a greater than fifty only three terms are needed, and for r/a greater than five hundred two terms suffice.

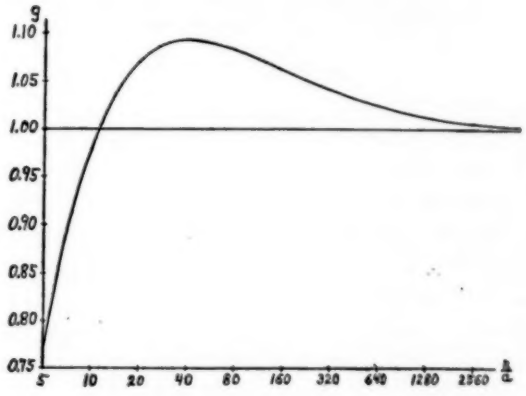

FIG. 1. Value of the function g.

We have calculated g for a number of values of r/a from both the "near" formula (12) and the "far" formula (14) for the purpose of showing the excellence of the fit obtained. The results are included in Table I. It will be noticed that in the overlap extending from $r/a=3$ to $r/a=9$ inclusive, where both series converge satisfactorily, discrepancies are nowhere greater than two parts in ten thousand. Values of g calculated from (14) for larger values of r/a are also contained in the table.

In Fig. 1 we have plotted the function g against the logarithm of r/a, to illustrate how the function behaves in the range $r=5a$ to $r=2560a$. Beyond the latter point the curve oscillates about the straight line $g=1$ with ever decreasing amplitude. The function g becomes unity first at $r=11.18a$, again at $r=9426a$, and next at $r=7{,}389{,}000a$. In fact, $g=1$ for

$$r=9426a[783.9]^n, \quad (15)$$

where n is any positive integer including zero.

PHYSICAL REVIEW VOLUME 68, NUMBERS 5 AND 6 SEPTEMBER 1 AND 15, 1945

Equations of Motion for Classical Dynamical Systems of Variable Mass*

JOSEPH GIARRATANA
U. S. Naval Academy, Annapolis, Maryland
(Received March 9, 1945)

A set of general equations of motion for classical dynamical systems of variable mass is derived. The variation of mass may be caused by either a continuous deformation and motion of the defining surface or a motion of the material points of the system, or both. Special cases of the general equations are also considered.

PART 1

IN the discussion which follows, the term, dynamical system, S, will be used to denote the totality of those material points which lie within an arbitrarily chosen finite closed surface S. Neither the shape of the surface nor the volume V which it encloses need be independent of the time. The position vector $\mathbf{q}_v$ of the centroid of the volume V relative to the origin 0 of an inertial reference triple $(\mathbf{i}, \mathbf{j}, \mathbf{k})$ may also vary with the time. We shall, however, restrict ourselves to the discussion of systems such that, during a given time interval $a \leq t \leq b$, each point of the defining surface has a position vector which, together with its first two time derivatives, is a continuous function of the time. As a consequence of this restriction, the centroidal vector $\mathbf{q}_v$ and its first two time derivatives will also be continuous with respect to the time.

We should note carefully the distinction between the centroidal vector $\mathbf{q}_v$ of the volume V and the centroidal vector $\mathbf{q}$ of the mass M which comprises the system. For the purpose of clarifying this distinction, there is represented in Fig. 1 a system for which these two vectors are not equal. Here the surface $ABCD$ comprises the surface S which defines the system. All of the mass M is contained within the shaded portion of the volume V. From the usual definitions of the centroids of masses and volumes, it follows, at once, that the centroidal vectors $\mathbf{q}_v$ and $\mathbf{q}$ are unequal. The latter vector we shall refer to as the centroidal vector of the system.

For the purposes of the present paper, it is convenient to divide dynamical systems into two classes. The first of these comprises all those systems whose total mass remains constant; the second, those whose total mass varies with the time. Systems of the first class may be divided further into two subclasses. In the first subclass we place those systems whose mass, while constant in magnitude, does not retain its identity. In the second subclass, on the other hand, we place those systems whose mass not only remains constant but retains its identity as well. A system of each of these subclasses is illustrated in Figs. 2 and 3, respectively. In each of these figures, R represents a rigid uniform rectilinear distribution of matter whose velocity $\mathbf{v}_R$ has a direction parallel to R itself. For both systems the defining surface S is rigid and, therefore, of

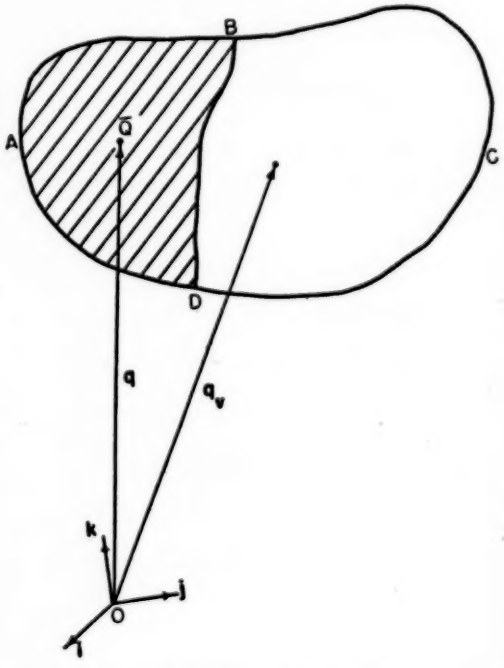

FIG. 1. System in which the centroidal vector $\mathbf{q}_v$ is not equal to the vector $\mathbf{q}$.

* The opinions or assertions contained in this paper are the private ones of the writer and are not to be construed as official or reflecting the views of the Navy Department or the naval service at large.

constant shape. The surface S of Fig. 2 has a velocity $\mathbf{v}_S$ which is equal to $-\mathbf{v}_R$. In accordance with our definition, the dynamical system represented in this figure comprises all of the material points of R which are situated within the surface S. Obviously, as long as neither of the ends of R lies within S, the mass M of the system remains constant. The material points which comprise the system, however, are changing continually. This system belongs, therefore, to the first of our subclasses. The surface S which defines the system of Fig. 3 moves with a velocity $\mathbf{v}_S$ which is equal to $+\mathbf{v}_R$. Consequently, the material points which comprise this system do not change with the time, i.e., the mass of the system retains its identity. We have, accordingly, a system of the second subclass.

The translational equation of motion for systems belonging to the second subclass is the well-known equation $\sum_i \mathbf{F}_i = M\mathbf{A}$. In this equation the summation $\sum_i \mathbf{F}_i$ represents the sum of the external forces, that is, the sum of those forces which arise from sources external to the defining surface S. The vector $\mathbf{A}$ is the acceleration vector for the centroid of the system. It is the purpose of the first portion of this paper to present the derivation of an analogous translational equation of motion of considerable generality for the class of dynamical systems whose mass is variable.

We shall begin our derivation by considering three related systems S, S_1, and S_2 whose descriptions follow. The system S is the system for which a translational equation of motion is to be derived. In the time interval $a \leq t \leq b$ the mass M of this system is assumed to be (a) finite and unequal to zero, (b) monotonic with respect to the time, and (c) a continuous function of the time together with its first and second time derivatives. Suppose now that the value of M corresponding to some arbitrarily chosen interior point t_1 of the interval $a \leq t \leq b$ is M_2 and suppose, further, that the material points comprising the system at this instant are identified so that their motion previous and subsequent to this instant may be studied. These material points comprise a second system S_2 whose mass not only remains constant and equal to M_2 but retains its identity as well. For this system, then, the equation of motion is

$$\mathbf{F}_2(t_1; t) = M_2(t_1) \cdot \mathbf{A}_2(t_1; t). \tag{1}$$

In this equation and, indeed, throughout the ensuing discussion, the time t_1 plays the role of a parameter. The symbol $\mathbf{F}_2(t_1; t)$ represents the sum of the external forces acting upon the system S_2 at the time t. To indicate that the various

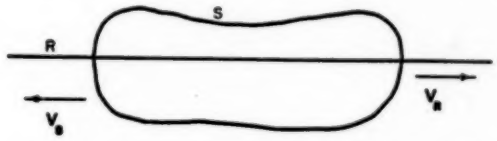

FIG. 2. System of constant mass, but the mass does not retain its identity.

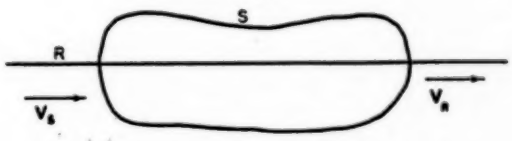

FIG. 3. System of constant and identical mass.

quantities which appear in this equation are those associated with the system S_2 we have used the subscript 2. For the two systems S and S_2 we shall make the assumption that at all points of the interval $a \leq t \leq b$ except $t = t_1$, either (a), the material points of S_2 comprise a proper subset of the material points of S, or (b), the material points of S comprise a proper subset of the material points of S_2. In accordance with this assumption, if t is unequal to t_1, one or the other of the relations,

$$M(t) = M_2(t_1) + M_1(t_1; t), \quad (M > M_2), \tag{2a}$$

$$M(t) = M_2(t_1) - M_1(t_1; t), \quad (M < M_2), \tag{2b}$$

will be valid. In these relations the symbol $M_1(t_1; t)$ represents the mass of those material points which together with the material points of the system S_2 or the system S comprise, respectively, the material points of the system S or the system S_2. These material points, of total mass M_1, comprise the remaining one of the three systems S, S_1, and S_2. The situation corresponding to Eq. (2a) is represented graphically in Fig. (4a); that corresponding to (2b), in Fig. (4b). In each of these two figures, $ABCDA$, $ABCEA$, and $AECDA$ represent the surfaces S, S_1, and S_2, respectively. Taken in the same order these surfaces define systems of mass M, M_1, and M_2.

During the time interval $a \leq t \leq b$ both $M(t)$ and $M_2(t_1)$ are continuous functions of the time t

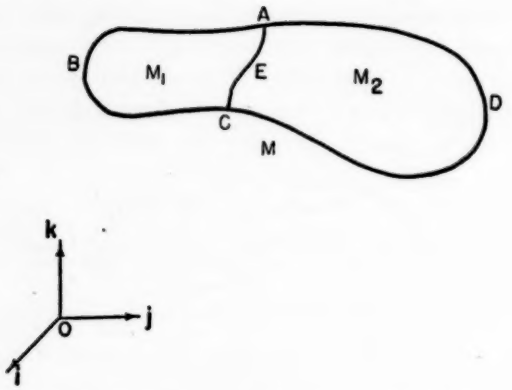

FIG. 4a. A system corresponding to Eq. (2a).

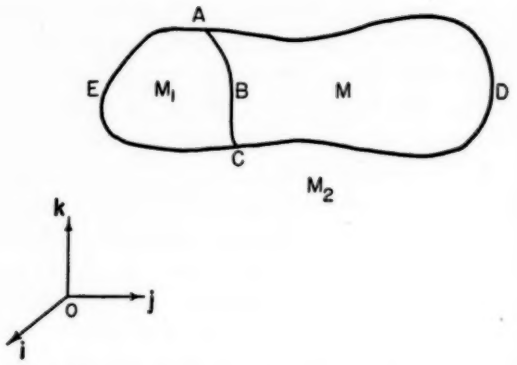

FIG. 4b. A system corresponding to Eq. (2b).

and have continuous first and second time derivatives. Accordingly, their difference $M-M_2$ has the same properties. We shall denote this function by the symbol φ. By definition, then,

$$\varphi(t_1;t)\equiv M(t)-M_2(t_1), \quad (a\leq t\leq b). \tag{3a}$$

As a consequence of this definition and the Eqs. (2a) and (2b), we have the further relations

$$\varphi'(t)=M'(t), \quad (a\leq t\leq b); \tag{3b}$$

$$\varphi''(t)=M''(t), \quad (a\leq t\leq b); \tag{3c}$$

$$\varphi(t_1;t)=M_1(t_1;t), \quad (M>M_2); \tag{3d}$$

$$\varphi(t_1;t_1)=M_1(t_1;t_1)=0, \quad (M=M_2); \tag{3e}$$

$$\varphi(t_1;t)=-M_1(t_1;t), \quad (M<M_2). \tag{3f}$$

The primes in Eqs. (3b) and (3c) indicate differentiation with respect to the time t. It will be noted that in these two equations the parameter t_1 does not appear.

We consider next the centroidal vectors $\mathbf{q}(t)$, $\mathbf{r}_1(t_1;t)$, and $\mathbf{p}(t_1;t)$ of the systems S, S_1, and S_2, respectively. These three vectors are defined by the relations

$$\mathbf{q}(t)\equiv\frac{\int_S \mathbf{c}\,dm}{\int_S dm}=\frac{\int_S \mathbf{c}\,dm}{M}, \tag{4a}$$

$$\mathbf{r}_1(t_1;t)\equiv\frac{\int_{S_1} \mathbf{c}\,dm}{\int_{S_1} dm}=\frac{\int_{S_1} \mathbf{c}\,dm}{M_1}, \tag{4b}$$

$$\mathbf{p}(t_1;t)\equiv\frac{\int_{S_2} \mathbf{c}\,dm}{\int_{S_2} dm}=\frac{\int_{S_2} \mathbf{c}\,dm}{M_2}. \tag{4c}$$

The symbols dm and $\mathbf{c}$ represent the differential of mass and its position vector, respectively, while the subscripts S, S_1, and S_2 indicate the systems for which the corresponding integrals are to be evaluated. As a consequence of the properties of M, M_2 and the surfaces which define our dynamical systems, it follows that $\mathbf{q}$ and $\mathbf{p}$ are continuous functions of the time t and possess continuous first and second time derivatives throughout the given time interval $a\leq t\leq b$. A similar statement is not true for the centroidal vector $\mathbf{r}_1$, for at the instant t_1 the mass M_1 is zero, and $\mathbf{r}_1$ and its time derivatives are undefined. We shall restrict the properties of $\mathbf{r}_1$ further by making the following assumptions:

(*a*) The vector $\lim_{t\to t_1}\mathbf{r}_1(t_1;t)$ exists. We shall denote this vector by the symbol $\mathbf{b}(t_1)$.

(*b*) The vector $\lim_{t\to t_1}\mathbf{r}_1'(t_1;t)$ exists and is finite. This vector we shall represent by the symbol $\mathbf{w}(t_1)$.

(*c*) The vectors $\lim_{t\to(t_1-0)}\mathbf{r}_1''(t_1;t)$ and $\lim_{t\to(t_1+0)}\mathbf{r}_1''(t_1;t)$ exist and are finite.

From the fact that the systems to which we restrict ourselves are bounded by finite closed surfaces, it follows that the vector $\mathbf{b}(t_1)$ is finite. At all points of the interval $a\leq t\leq b$ except t_1 the vector $\mathbf{r}_1$ and its first two time derivatives are

continuous functions of the time. This follows as a consequence of the properties of M, M_2 and the surfaces which define our systems.

Turning now to the various moments of mass, we find that in consequence of the properties of M, M_2, $\mathbf{q}$, and $\mathbf{p}$, the two moments $M_2\mathbf{p}$ and $M\mathbf{q}$ are, together with their first two time derivatives, continuous functions of the time t throughout the interval $a \leq t \leq b$. The moment $M_1\mathbf{r}_1$, on the other hand, is discontinuous together with its first two time derivatives at the point t_1. These three moments are related according to the equations

$$M_2(t_1)\cdot\mathbf{p}(t_1;t) = M(t)\cdot\mathbf{q}(t) - M_1(t_1;t)\cdot\mathbf{r}_1(t_1;t), \quad (M > M_2); \tag{5a}$$

$$M_2(t_1)\cdot\mathbf{p}(t_1;t_1) = M(t_1)\cdot\mathbf{q}(t_1), \quad (M = M_2); \tag{5b}$$

$$M_2(t_1)\cdot\mathbf{p}(t_1;t) = M(t)\cdot\mathbf{q}(t) + M_1(t_1;t)\cdot\mathbf{r}_1(t_1;t), \quad (M < M_2). \tag{5c}$$

Upon introducing the function φ which we defined above and a vector function $\mathbf{r}$ whose definition will follow, these three relations may be replaced by the single equivalent relation

$$M_2(t_1)\cdot\mathbf{p}(t_1;t) = M(t)\cdot\mathbf{q}(t) - \varphi(t_1;t)\cdot\mathbf{r}(t_1;t), \quad (a \leq t \leq b). \tag{6}$$

The vector $\mathbf{r}$ is defined as follows:

(a) For $t \neq t_1$,

$$\mathbf{r}(t_1;t) \equiv \mathbf{r}_1(t_1;t);$$

(b) For $t = t_1$,

$$\mathbf{r}(t_1;t_1) \equiv \mathbf{b}(t_1) \equiv \operatorname*{Lim}_{t\to t_1} \mathbf{r}_1(t_1;t);$$

$$\mathbf{r}'(t_1;t_1) \equiv \mathbf{w}(t_1) \equiv \operatorname*{Lim}_{t\to t_1} \mathbf{r}_1'(t_1;t);$$

$\mathbf{r}''(t_1;t_1)$ is finite but otherwise arbitrary. From its definition it follows that the vector function $\mathbf{r}$ and its first time derivative are continuous at every point of the given time interval. As will be seen presently our derivation of the translational equation of motion for the system S does not require the function $\mathbf{r}''$ to be continuous at the point t_1.

It is worth noting that although the function $\mathbf{r}''$ may be discontinuous at the point t_1 the function $(\varphi\cdot\mathbf{r})''$ is continuous at this point. This may be proved very easily. Thus, making use of the continuity of the functions φ, φ', φ'', $\mathbf{r}$ and $\mathbf{r}'$ at the point t_1, we have at once

$$\begin{aligned}\operatorname*{Lim}_{t\to t_1}[\varphi(t_1;t)\cdot\mathbf{r}(t_1;t)]'' &= \operatorname*{Lim}_{t\to t_1}[\varphi''(t)\cdot\mathbf{r}(t_1;t)+2\varphi'(t)\cdot\mathbf{r}'(t_1;t)+\varphi(t_1;t)\cdot\mathbf{r}''(t_1;t)]\\ &= \varphi''(t_1)\cdot\mathbf{r}(t_1;t_1)+2\varphi'(t_1)\cdot\mathbf{r}'(t_1;t_1)+[\varphi(t_1;t_1)\cdot\operatorname*{Lim}_{t\to t_1}\mathbf{r}''(t_1;t)]\\ &= M''(t_1)\cdot\mathbf{b}(t_1)+2M'(t_1)\cdot\mathbf{w}(t_1)+[\varphi(t_1;t_1)\cdot\operatorname*{Lim}_{t\to t_1}\mathbf{r}_1''(t_1;t)].\end{aligned}$$

Since both of the possible values of the vector $\operatorname*{Lim}_{t\to t_1}\mathbf{r}_1''(t_1;t)$ are finite and since the scalar $\varphi(t_1;t_1)$ is equal to zero, it follows that the bracketed product on the right is a zero vector. Consequently we may write, simply,

$$\operatorname*{Lim}_{t\to t_1}[\varphi(t_1;t)\cdot\mathbf{r}(t_1;t)]'' = M''(t_1)\cdot\mathbf{b}(t_1)+2M'(t_1)\cdot\mathbf{w}(t_1). \tag{7}$$

If now, we evaluate the function $[\varphi\cdot\mathbf{r}]''$ at the point t_1 we obtain the equation

$$\begin{aligned}\{[\varphi(t_1;t)\cdot\mathbf{r}(t_1;t)]''\}_{t=t_1} &= [\varphi''(t_1)\cdot\mathbf{r}(t_1;t_1)+2\varphi'(t_1)\cdot\mathbf{r}'(t_1;t_1)+\varphi(t_1;t_1)\cdot\mathbf{r}''(t_1;t_1)]\\ &= M''(t_1)\cdot\mathbf{b}(t_1)+2M'(t_1)\cdot\mathbf{w}(t_1)+\varphi(t_1;t_1)\cdot\mathbf{r}''(t_1;t_1).\end{aligned}$$

Upon recalling, once more, that $\varphi(t_1;t_1)$ equals zero and that $\mathbf{r}''(t_1;t_1)$ is finite, we see that the third term on the right side of this relation also vanishes. We may, therefore, write

$$\{[\varphi(t_1;t)\cdot\mathbf{r}(t_1;t)]''\}_{t=t_1} = M''(t_1)\cdot\mathbf{b}(t_1)+2M'(t_1)\cdot\mathbf{w}(t_1). \tag{8}$$

The right sides of relations (7) and (8) are identical. Consequently,

$$\operatorname*{Lim}_{t\to t_1}\{[\varphi(t_1;t)\cdot\mathbf{r}(t_1;t)]''\} = \{[\varphi(t_1;t)\cdot\mathbf{r}(t_1;t)]''\}_{t=t_1}, \tag{9}$$

and the continuity of $[\varphi\cdot\mathbf{r}]''$ at the point t_1 is established.

Differentiation of both sides of Eq. (6) twice with respect to the time yields the relation

$$M_2(t_1)\cdot\mathbf{p}''(t_1;t)=[M''(t)\cdot\mathbf{q}(t)+2M'(t)\cdot\mathbf{q}'(t)+M(t)\cdot\mathbf{q}''(t)]$$
$$-[\varphi''(t)\cdot\mathbf{r}(t_1;t)+2\varphi'(t)\cdot\mathbf{r}'(t_1;t)+\varphi(t_1;t)\cdot\mathbf{r}''(t_1;t)], \quad (10)$$

which is valid throughout the interval $a\leq t\leq b$. The vector $\mathbf{p}''$ is, of course, the acceleration vector $\mathbf{A}_2$ of the centroid of the system S_2. In accordance with Eq. (1), therefore, we may replace the left side of (10) with the summation of the external forces acting upon the system S_2. With this substitution Eq. (10) becomes

$$\mathbf{F}_2(t_1;t)=[M''(t)\cdot\mathbf{q}(t)+2M'(t)\cdot\mathbf{q}'(t)+M(t)\cdot\mathbf{q}''(t)]$$
$$-[\varphi''(t)\cdot\mathbf{r}(t_1;t)+2\varphi'(t)\cdot\mathbf{r}'(t_1;t)+\varphi(t_1;t)\cdot\mathbf{r}''(t_1;t)], \quad (a\leq t\leq b). \quad (11)$$

Worthy of note is the fact that whenever $M>M_2$ the summation $\mathbf{F}_2(t_1;t)$ must include the forces of interaction between the systems S_1 and S_2. In consequence of relation (8) the form taken by this equation when $t=t_1$ is

$$\mathbf{F}_2(t_1;t_1)=[M''(t_1)\cdot\mathbf{q}(t_1)+2M'(t_1)\cdot\mathbf{q}'(t_1)+M(t_1)\cdot\mathbf{q}''(t_1)]$$
$$-[M''(t_1)\cdot\mathbf{b}(t_1)+2M'(t_1)\cdot\mathbf{w}(t_1)], \quad (a<t_1<b). \quad (12)$$

At this instant, moreover, the forces which act upon the system S_2 are identical with those which act upon the system S. In consequence we may replace the left side of (12) with the summation $\mathbf{F}(t_1)$ of the external forces acting upon the system S at the time t_1. After making this substitution and deleting the subscript, 1, we obtain, finally, the equation

$$\mathbf{F}(t)=[M''(t)\cdot\mathbf{q}(t)+2M'(t)\cdot\mathbf{q}'(t)+M(t)\cdot\mathbf{q}''(t)]-[M''(t)\cdot\mathbf{b}(t)+2M'(t)\cdot\mathbf{w}(t)], \quad (a<t<b). \quad (13)$$

This equation comprises one form of the translational differential equation of motion of the system S. Another form, in which the momentum $\mathbf{L}(t)$ of the system S appears explicitly, may be obtained very easily. If we differentiate Eq. (6) once with respect to the time we obtain the relation

$$M_2(t_1)\cdot\mathbf{p}'(t_1;t)=[M'(t)\cdot\mathbf{q}(t)+M(t)\cdot\mathbf{q}'(t)]-[\varphi'(t)\cdot\mathbf{r}(t_1;t)+\varphi(t_1;t)\cdot\mathbf{r}'(t_1;t)], \quad (a\leq t\leq b). \quad (14)$$

The left side of this equation represents the linear momentum $\mathbf{L}_2(t_1;t)$ of the system S_2 at the time t. For the momentum $\mathbf{L}_2$, then, we have the formula

$$\mathbf{L}_2(t_1;t)=[M'(t)\cdot\mathbf{q}(t)+M(t)\cdot\mathbf{q}'(t)]-[\varphi'(t)\cdot\mathbf{r}(t_1;t)+\varphi(t_1;t)\cdot\mathbf{r}'(t_1;t)], \quad (a\leq t\leq b). \quad (15)$$

Since $\varphi(t_1;t_1)=0$ and $\mathbf{r}'(t_1;t_1)$ is a finite vector, it follows that the product $\varphi(t_1;t_1)\cdot\mathbf{r}'(t_1;t_1)$ represents a zero vector. For $t=t_1$, therefore, Eq. (15) takes the form

$$\mathbf{L}_2(t_1;t_1)=[M'(t_1)\cdot\mathbf{q}(t_1)+M(t_1)\cdot\mathbf{q}'(t_1)]-[\varphi'(t_1)\cdot\mathbf{r}(t_1;t_1)]$$
$$=[M'(t_1)\cdot\mathbf{q}(t_1)+M(t_1)\cdot\mathbf{q}'(t_1)]-[M'(t_1)\cdot\mathbf{b}(t_1)], \quad (a<t_1<b). \quad (16)$$

For this instant, moreover, the linear momenta $\mathbf{L}(t_1)$ and $\mathbf{L}_2(t_1;t_1)$ are equal. In consequence we may replace the left side of (16) with $\mathbf{L}(t_1)$. This substitution, together with a deletion of the subscript, 1, yields for the momentum $\mathbf{L}(t)$ of the system S the formula

$$\mathbf{L}(t)=[M'(t)\cdot\mathbf{q}(t)+M(t)\cdot\mathbf{q}'(t)]-[M'(t)\cdot\mathbf{b}(t)], \quad (a<t<b). \quad (17)$$

The time rate of change of $\mathbf{L}$ obeys the relation

$$\mathbf{L}'(t)=[M''(t)\cdot\mathbf{q}(t)+2M'(t)\cdot\mathbf{q}'(t)+M(t)\cdot\mathbf{q}''(t)]-[M''(t)\cdot\mathbf{b}(t)+M'(t)\cdot\mathbf{u}(t)], \quad (a<t<b). \quad (18)$$

where the vector $\mathbf{u}(t)$ is defined by the relation

$$\mathbf{u}(t)\equiv\mathbf{b}'(t). \quad (19)$$

Upon comparing Eqs. (18) and (13) we see that the latter may be replaced by the equivalent relation

$$\mathbf{F}(t)=\mathbf{L}'(t)+[\mathbf{u}(t)-2\mathbf{w}(t)]\cdot M'(t), \quad (a<t<b). \tag{20}$$

For many applications this form of the translational equation of motion will be found to be more convenient than the form (13).

Strictly speaking, we have demonstrated the validity of Eqs. (13), (17), and (20) only for interior points of the interval $a\leq t\leq b$. If t_1 is an end point of the interval a more or less obvious modification of the above arguments leads to the same results. These equations are valid, therefore, throughout the interval $a\leq t\leq b$.

PART 2

We shall derive now an equation which connects the moment of the external forces relative to an arbitrary fixed point and the time derivative of the angular momentum of the system relative to the same point. Let a fixed point J be chosen and let $\mathbf{H}(t)$, $\mathbf{H}_1(t_1;t)$, and $\mathbf{H}_2(t_1;t)$ denote, respectively, the angular momenta of the systems S, S_1, and S_2 relative to this point. The latter systems are defined in the same manner as in the derivation of the translational differential equation of motion. At any instant in the interval $a\leq t\leq b$ these momenta will be related by one of the following equations:

$$\mathbf{H}_2(t_1;t)=\mathbf{H}(t)-\mathbf{H}_1(t_1;t), \quad (M>M_2); \tag{21a}$$

$$\mathbf{H}_2(t_1;t_1)=\mathbf{H}(t_1), \quad (M=M_2); \tag{21b}$$

$$\mathbf{H}_2(t_1;t)=\mathbf{H}(t)+\mathbf{H}_1(t_1;t), \quad (M<M_2). \tag{21c}$$

We shall assume that $\mathbf{H}(t)$ and $\mathbf{H}_2(t_1;t)$ are continuous functions of the time t, and that they possess continuous first time derivatives in the interval $a\leq t\leq b$. As a consequence of these assumptions the difference $\mathbf{H}-\mathbf{H}_2$ will have the same properties. Upon denoting this vector function by the symbol $\mathbf{h}$ we may write immediately

$$\mathbf{H}_2(t_1;t)\equiv\mathbf{H}(t)-\mathbf{h}(t_1;t), \quad (a\leq t\leq b). \tag{22a}$$

From this defining relation and the relations (21a)–(21c), we may deduce readily the validity of the following equations:

$$\mathbf{H}_2'(t_1;t)=\mathbf{H}'(t)-\mathbf{h}'(t_1;t), \quad (a\leq t\leq b); \tag{22b}$$

$$\mathbf{h}(t_1;t)=\mathbf{H}_1(t_1;t), \quad (M>M_2); \tag{22c}$$

$$\mathbf{h}(t_1;t_1)=\mathbf{H}_1(t_1;t_1)=\mathbf{0}, \quad (M=M_2); \tag{22d}$$

$$\mathbf{h}(t_1;t)=-\mathbf{H}_1(t_1;t), \quad (M<M_2). \tag{22e}$$

The primes in Eq. (22b) indicate differentiation with respect to the variable t. Since the system S_2 is one whose mass not only remains constant but retains its identity as well, the quantity $\mathbf{H}_2'$ satisfies the well-known relation

$$\mathbf{K}_2(t_1;t)=\mathbf{H}_2'(t_1;t).$$

Here $\mathbf{K}_2$ indicates the total moment, taken relative to the fixed point J, of the external forces acting on the system S_2. Upon eliminating $\mathbf{H}_2'$ between this equation and Eq. (22b) we obtain the relation

$$\mathbf{K}_2(t_1;t)=\mathbf{H}'(t)-\mathbf{h}'(t_1;t), \quad (a\leq t\leq b). \tag{23}$$

When $t=t_1$, the forces acting upon the system S are identical with those acting upon the system S_2. For this instant, therefore, the moments of these two sets of forces relative to the point J are equal, and Eq. (23) may be replaced with the relation

$$\mathbf{K}(t_1)=\mathbf{H}'(t_1)-\boldsymbol{\lambda}(t_1), \quad (a<t_1<b). \tag{24}$$

In this equation $\mathbf{K}(t_1)$ denotes the moment, relative to the point J, of the external forces acting on the system S at the time t_1. The quantity $\boldsymbol{\lambda}(t_1)$ is defined as follows:

$$\left.\begin{aligned}&\boldsymbol{\lambda}(t_1)\equiv\mathbf{h}'(t_1;t_1)=\lim_{t\to t_1}[\mathbf{H}_1'(t_1;t)]\\ &\text{if } M>M_2 \text{ during the approach to the limit;}\\ &\boldsymbol{\lambda}(t_1)\equiv\mathbf{h}'(t_1;t_1)=\lim_{t\to t_1}[-\mathbf{H}_1'(t_1;t)]\\ &\text{if } M<M_2 \text{ during the approach to the limit.}\end{aligned}\right\} \tag{25}$$

If t_1 is an end point of the interval $a\leq t\leq b$, we can modify the above argument slightly and obtain again the results (24) and (25). Inasmuch as the parameter t_1 represents an arbitrary point of the interval $a\leq t\leq b$, we may drop the subscripts and write, more simply,

$$\mathbf{K}(t)=\mathbf{H}'(t)-\boldsymbol{\lambda}(t), \quad (a\leq t\leq b). \tag{26}$$

This equation comprises the second of the equa-

tions of motion which we wished to derive. We shall refer to it as the rotational equation of motion.

PART 3

The argument used in the derivation of Eq. (26) may be employed also in connection with the linear momenta $\mathbf{L}(t)$, $\mathbf{L}_1(t_1;t)$ and $\mathbf{L}_2(t_1;t)$ of the systems S, S_1 and S_2, respectively. The result will be an alternative form of the translational equation of motion. Corresponding to the Eqs. (21a)–(21c), we shall have now the equations:

$$\mathbf{L}_2(t_1;t)=\mathbf{L}(t)-\mathbf{L}_1(t_1;t), \quad (M>M_2); \quad (27a)$$

$$\mathbf{L}_2(t_1;t_1)=\mathbf{L}(t_1), \quad (M=M_2); \quad (27b)$$

$$\mathbf{L}_2(t_1;t)=\mathbf{L}(t)+\mathbf{L}_1(t_1;t), \quad (M<M_2). \quad (27c)$$

We shall assume that with respect to the time t the momenta $\mathbf{L}$ and $\mathbf{L}_2$ are continuous functions and possess continuous first derivatives throughout the given interval. The difference of these two momenta comprises a function $\mathbf{l}(t_1;t)$ which possesses the same properties. Corresponding to Eqs. (22a)–(22e), the equations now are:

$$\mathbf{L}_2(t_1;t)\equiv\mathbf{L}(t)-\mathbf{l}(t_1;t), \quad (a\leq t\leq b); \quad (28a)$$

$$\mathbf{L}_2'(t_1;t)=\mathbf{L}'(t)-\mathbf{l}'(t_1;t), \quad (a\leq t\leq b); \quad (28b)$$

$$\mathbf{l}(t_1;t)=\mathbf{L}_1(t_1;t), \quad (M>M_2); \quad (28c)$$

$$\mathbf{l}(t_1;t_1)=\mathbf{L}_1(t_1;t_1)=\mathbf{o}, \quad (M=M_2); \quad (28d)$$

$$\mathbf{l}(t_1;t)=-\mathbf{L}_1(t_1;t), \quad (M<M_2). \quad (28e)$$

Inasmuch as the momentum $\mathbf{L}_2$ obeys the relation

$$\mathbf{F}_2(t_1;t)=\mathbf{L}_2'(t_1;t),$$

where $\mathbf{F}_2$ is the sum of the external forces acting upon the system S_2, we may replace Eq. (28b) with the equation

$$\mathbf{F}_2(t_1;t)=\mathbf{L}'(t)-\mathbf{l}'(t_1;t), \quad (a\leq t\leq b). \quad (29)$$

For the instant t_1 the sum of the forces acting upon the system S_2 will be equal to the sum of those acting upon the system S. Upon denoting the latter sum by the symbol $\mathbf{F}(t_1)$ we may replace Eq. (29) for this instant with the equation

$$\mathbf{F}(t_1)=\mathbf{L}'(t_1)-\mathbf{n}(t_1), \quad (a<t_1<b). \quad (30)$$

The symbol $\mathbf{n}(t)$ which appears in this relation is defined as follows:

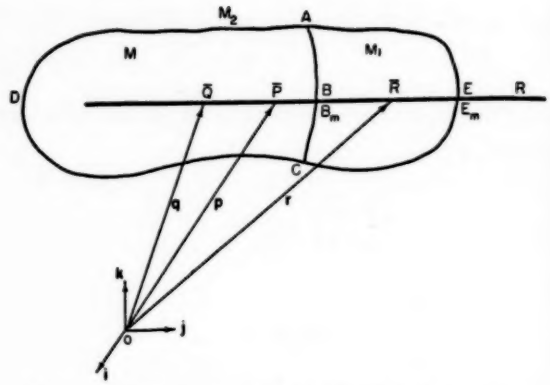

FIG. 5. One-dimensional distribution (R) of matter.

$$\left.\begin{aligned}&\mathbf{n}(t_1)\equiv\mathbf{l}'(t_1;t_1)=\lim_{t\to t_1}[\mathbf{L}_1'(t_1;t)]\\&\text{if } M>M_2 \text{ during the approach to the limit;}\\&\mathbf{n}(t_1)\equiv\mathbf{l}'(t_1;t_1)=\lim_{t\to t_1}[-\mathbf{L}_1'(t_1;t)]\\&\text{if } M<M_2 \text{ during the approach to the limit.}\end{aligned}\right\} \quad (31)$$

The modified argument which must be employed when t_1 is an end point of the given interval $(a\leq t\leq b)$ leads to the same results (30) and (31). Upon dropping the subscripts, as usual, we may write

$$\mathbf{F}(t)=\mathbf{L}'(t)-\mathbf{n}(t), \quad (a\leq t\leq b). \quad (32)$$

This equation comprises an alternative form of the translational equation of motion (20).

PART 4

When used in connection with the kinetic energies $T(t)$, $T_1(t_1;t)$ and $T_2(t_1;t)$ of the systems S, S_1, and S_2, respectively, the same argument leads to the following equation:

$$P(t_1)=T'(t_1)-\mu(t_1), \quad (a\leq t_1\leq b). \quad (33)$$

The symbol $P(t_1)$ represents the power of all the forces, both internal and external, acting upon the system S at the instant t_1. For the function $\mu(t_1)$, we have the following defining relations:

$$\left.\begin{aligned}&\mu(t_1)\equiv\lim_{t\to t_1}[T_1'(t_1;t)]\\&\text{if } M>M_2 \text{ during the approach to the limit.}\\&\mu(t_1)\equiv\lim_{t\to t_1}[-T_1'(t_1;t)]\\&\text{if } M<M_2 \text{ during the approach to the limit.}\end{aligned}\right\} \quad (34)$$

If we drop the subscripts from (33), we obtain the

equality

$$P(t)=T'(t)-\mu(t), \quad (a\leq t\leq b). \tag{35}$$

In contrast with our previously derived Eqs. (13), (20), (26) and (32), this is a scalar rather than a vector equation.

PART 5

We shall derive next a useful one-dimensional form of the translational equation. In Fig. 5, R represents a one-dimensional distribution of matter whose linear density ρ is an analytic function of the time t and the distance ξ from the material point E_m. The surfaces $ABCDA$, $ABCEA$, and $AECDA$ comprise the surfaces S, S_1, and S_2, respectively. We shall assume that during the interval $a\leq t\leq b$ all material points which pass through the surface S do so at the point B of this surface. In general, the velocity $\mathbf{v}_B$ of the point B will not be equal to the velocity $\mathbf{v}_{B_m}$ of the material point B_m with which it coincides. The material point with which B coincides at the time t_1 is the point which we have referred to already as E_m. We choose the surface S_2 so that its point E moves in coincidence with the particular material point E_m. This surface defines, therefore, a system whose mass remains constant and retains its identity, i.e., a system of the second subclass. The symbols $\bar{Q}$, $\bar{R}$ and $\bar{P}$ denote, in this order, the centroids of the systems S, S_1, and S_2. For the remaining symbols in Fig. 5, the meanings are the same as in the previous portions of this paper. When $t=t_1$ the vectors $\mathbf{OB}(t)$, $\mathbf{r}(t_1;t)$ and $\mathbf{OE}_m(t_1;t)$ are equal. Since, by definition, $\mathbf{r}(t_1;t_1)\equiv\mathbf{b}(t_1)$, we see that for this instant we may write

$$\mathbf{b}(t_1)=\mathbf{OB}(t_1).$$

Inasmuch as t_1 is an arbitrary point of the interval $a<t<b$, it follows that the vectors $\mathbf{b}$ and $\mathbf{OB}$ are equal to each other at every point of this interval. Accordingly, we may drop the subscript and write simply,

$$\mathbf{b}(t)=\mathbf{OB}(t).$$

Differentiation of this equation with respect to the time gives for the vector $\mathbf{u}(t)\equiv\mathbf{b}'(t)$ the result

$$\mathbf{u}(t)\equiv\mathbf{b}'(t)=\mathbf{v}_B(t), \tag{36}$$

where $\mathbf{v}_B$ is the velocity of the point B.

The vector $\mathbf{w}(t)$ may be obtained in the following manner. Let the position vector of the centroid $\bar{R}$ relative to the point E be denoted by the symbol $\mathbf{n}(t_1;t)$. The vector $\mathbf{r}$ may then be expressed in the form

$$\mathbf{r}(t_1;t)=\mathbf{OE}(t_1;t)+\mathbf{n}(t_1;t). \tag{37}$$

If, now, the reference triple $(\mathbf{i}, \mathbf{j}, \mathbf{k})$ has been chosen so that the vector $\mathbf{j}$ is parallel to R, the vector $\mathbf{n}$ may be replaced with the product $n\cdot\mathbf{j}$ in which n is the $\mathbf{j}$ scalar component of $\mathbf{n}$. With this substitution the equation for $\mathbf{r}$ becomes

$$\mathbf{r}(t_1;t)=\mathbf{OE}(t_1;t)+n(t_1;t)\cdot\mathbf{j}. \tag{38}$$

Upon differentiating both sides of this relation with respect to the time t we obtain the result

$$\begin{aligned}\mathbf{r}'(t_1;t)&=\mathbf{OE}'(t_1;t)+n'(t_1;t)\cdot\mathbf{j}\\&=\mathbf{v}_E(t_1;t)+n'(t_1;t)\cdot\mathbf{j}\end{aligned} \tag{39}$$

where $\mathbf{v}_E$ is the velocity of the point E and $n'\cdot\mathbf{j}$ is the velocity of the centroid $\bar{R}$ relative to E. In accordance with the definitions of $\mathbf{w}$ and $\mathbf{r}$ we may now write

$$\begin{aligned}\mathbf{w}(t_1)\equiv\mathbf{r}'(t_1;t_1)&=\lim_{t\to t_1}\mathbf{r}'(t_1;t)\\&=\mathbf{v}_E(t_1;t_1)+[\lim_{t\to t_1}n'(t_1;t)]\cdot\mathbf{j}.\end{aligned}$$

Since, according to our present definition of the surface S_2, the point E remains in coincidence with the material point E_m, it follows that the velocity $\mathbf{v}_E$ of E is equal to the velocity $\mathbf{v}_{E_m}$ of the point E_m. Furthermore, at the time $t=t_1$, the material point E_m is identical with the material point B_m. For this instant, therefore, we have the result that $\mathbf{v}_E=\mathbf{v}_{B_m}$. With this substitution the above relation for $\mathbf{w}$ becomes

$$\mathbf{w}(t_1)=\mathbf{v}_{B_m}(t_1)+[\lim_{t\to t_1}n'(t_1;t)]\cdot\mathbf{j}. \tag{40}$$

The scalar n obeys the defining relation

$$\begin{aligned}n(t_1;t)\int_{\beta(t_1;t)}^{0}\rho(t_1;\xi,t)d\xi&\\=\int_{\beta(t_1;t)}^{0}\xi\cdot\rho(t_1;\xi,t)d\xi,&\end{aligned} \tag{41}$$

in which β is the $\mathbf{j}$ scalar component of the vector $\mathbf{EB}$ from E to B. At any time t the density ρ may be expanded in a power series of the form

$$\begin{aligned}\rho(t_1;\xi,t)&=\rho(t_1;0,t)+\rho_1(t_1;0,t)\cdot\xi\\&\quad+\frac{\rho_2(t_1;0,t)\cdot\xi^2}{2!}+\cdots.\end{aligned} \tag{42}$$

In this relation the subscripts 1, 2, 3, $\cdots$ etc. placed upon the ρ's indicate the first, second, third, $\cdots$ etc. partial derivatives with respect to the variable ξ. Upon replacing ρ in relation (41) with its power series expansion and integrating the result term by term we arrive at the relation

$$-n(t_1;t)\cdot\left[\rho(t_1;0,t)\cdot\beta(t_1;t)+\rho_1(t_1;0,t)\cdot\frac{\beta^2(t_1;t)}{2}+\frac{\rho_2(t_1;0,t)}{2!}\cdot\frac{\beta^3(t_1;t)}{3}+\cdots\right]$$

$$=-\left[\rho(t_1;0,t)\cdot\frac{\beta^2(t_1;t)}{2}+\rho_1(t_1;0,t)\cdot\frac{\beta^3(t_1;t)}{3}+\frac{\rho_2(t_1;0,t)}{2!}\cdot\frac{\beta^4(t_1;t)}{4}+\cdots\right]$$

or, equally well,

$$n(t_1;t)\left[\rho(t_1;0,t)+\rho_1(t_1;0,t)\cdot\frac{\beta(t_1;t)}{2}+\frac{\rho_2(t_1;0,t)}{2!}\cdot\frac{\beta^2(t_1;t)}{3}+\cdots\right]$$

$$=\beta(t_1;t)\left[\frac{\rho(t_1;0,t)}{2}+\rho_1(t_1;0,t)\cdot\frac{\beta(t_1;t)}{3}+\frac{\rho_2(t_1;0,t)}{2!}\cdot\frac{\beta^2(t_1;t)}{4}+\cdots\right]. \quad (43)$$

If we differentiate both sides of this equation with respect to the time t we obtain the relation

$$n'(t_1;t)\left[\rho(t_1;0,t)+\rho_1(t_1;0,t)\cdot\frac{\beta(t_1;t)}{2}+\cdots\right]+n(t_1;t)\left[\rho'(t_1;0,t)+\left\{\rho_1'(t_1;0,t)\cdot\frac{\beta(t_1;t)}{2}\right.\right.$$

$$\left.\left.+\rho_1(t_1;0,t)\cdot\frac{\beta'(t_1;t)}{2}\right\}+\cdots\right]=\beta'(t_1;t)\left[\frac{\rho(t_1;0,t)}{2}+\rho_1(t_1;0,t)\cdot\frac{\beta(t_1;t)}{3}+\cdots\right]$$

$$+\beta(t_1;t)\left[\frac{\rho'(t_1;0,t)}{2}+\left\{\rho_1'(t_1;0,t)\cdot\frac{\beta(t_1;t)}{3}+\rho_1(t_1;0,t)\cdot\frac{\beta'(t_1;t)}{3}\right\}+\cdots\right]. \quad (44)$$

The limiting form of this equation as t approaches t_1 and n and β approach zero is

$$\{\operatorname*{Lim}_{t\to t_1} n'(t_1;t)\}\rho(t_1;0,t_1)=\{\operatorname*{Lim}_{t\to t_1}\beta'(t_1;t)\}\frac{\rho(t_1;0,t_1)}{2},$$

or,

$$\operatorname*{Lim}_{t\to t_1} n'(t_1;t)=\tfrac{1}{2}\operatorname*{Lim}_{t\to t_1}\beta'(t_1;t). \quad (45)$$

The limit on the right is simply the **j** scalar component of the velocity of the point B relative to the point E at the time t_1 when these points coincide. In consequence, we may write

$$\operatorname*{Lim}_{t\to t_1} n'(t_1;t)=\tfrac{1}{2}\operatorname*{Lim}_{t\to t_1}\beta'(t_1;t)=\tfrac{1}{2}[v_B(t_1)-v_E(t_1;t_1)]=\tfrac{1}{2}[v_B(t_1)-v_{B_m}(t_1)], \quad (46)$$

where v_B and v_{B_m} are the **j** scalar components of $\mathbf{v}_B$ and $\mathbf{v}_{B_m}$, respectively. In view of this result, we may replace the Eq. (40) for **w** with the equivalent relation

$$\mathbf{w}(t_1)=\mathbf{v}_{B_m}(t_1)+\tfrac{1}{2}[v_B(t_1)-v_{B_m}(t_1)]\cdot\mathbf{j}=\tfrac{1}{2}[\mathbf{v}_B(t_1)+\mathbf{v}_{B_m}(t_1)]. \quad (47)$$

Dropping the subscript 1, as usual, we have for the vector **w** at any point of the time interval $a\leq t\leq b$,

$$\mathbf{w}(t)=\tfrac{1}{2}[\mathbf{v}_B(t)+\mathbf{v}_{B_m}(t)]. \quad (48)$$

To obtain the desired one-dimensional form of the translational equation, we substitute into Eq. (20) the values of **u** and **w** given by relations (36) and (48) respectively. This substitution yields at once the relation

$$\mathbf{F}(t)=\mathbf{L}'(t)-\mathbf{v}_{B_m}(t)\cdot M'(t), \quad (a\leq t\leq b). \quad (49)$$

Because of its importance we recall once more the fact that $\mathbf{v}_{B_m}$ is the absolute velocity of the material points of R at the instant they cross the surface S. The forces $\mathbf{F}(t)$ must, of course, include the force of reaction at the point B.

PART 6

When the system under consideration is one all material points of which have the same common velocity $\mathbf{v}(t)$, the translational equation of motion has an especially simple form. Let us assume that as $t \to t_1$, the mass M is greater than the mass M_2. The quantity $\mathbf{n}$ which appears in (30) must then be calculated according to the first of the defining relations (31). We have

$$\mathbf{n}(t_1) = \lim_{t \to t_1} \mathbf{L}_1'(t_1; t) = \lim_{t \to t_1} [M_1'(t_1; t) \cdot \mathbf{v}(t) + M_1(t_1; t) \cdot \mathbf{v}'(t)]$$
$$= \lim_{t \to t_1} [M_1'(t_1; t) \cdot \mathbf{v}(t)] + 0 \cdot \mathbf{v}'(t_1). \tag{50}$$

In consequence of the relation

$$M(t) = M_2(t_1) + M_1(t_1; t), \quad (M > M_2), \tag{2a}$$

we must have

$$M'(t) = M_1'(t_1; t). \tag{51}$$

In accordance with this result, Eq. (50) may now be written in the form

$$\mathbf{n}(t_1) = \lim_{t \to t_1} [M'(t) \cdot \mathbf{v}(t)] = M'(t_1) \cdot \mathbf{v}(t_1). \tag{52}$$

The usual deletion of the subscripts gives us the more general relation

$$\mathbf{n}(t) = M'(t) \cdot \mathbf{v}(t), \quad (a \leq t \leq b). \tag{53}$$

Upon substituting this result in Eq. (32) we have

$$\mathbf{F}(t) = \mathbf{L}'(t) - \mathbf{n}(t) = [M'(t) \cdot \mathbf{v}(t) + M(t) \cdot \mathbf{v}'(t)] - M'(t) \cdot \mathbf{v}(t),$$

or, finally,

$$\mathbf{F}(t) = M(t) \cdot \mathbf{v}'(t), \quad (a \leq t \leq b). \tag{54}$$

This is the desired equation. Except for the fact that M is a function of the time, this relation is identical in form with the translational equation for systems of the second subclass. As usual, care must be taken to include in $\mathbf{F}(t)$ the forces of reaction between the system and the mass which is entering or leaving the system.

PART 7

In this, the final portion of this paper, we shall consider some of the factors involved in the choice of systems S, S_1, and S_2 which satisfy the assumed conditions.

Let us consider first the case presented by a system S whose change of mass throughout the time interval $a \leq t \leq b$ is caused by a flow of matter through a single region σ of its defining surface. In particular, we shall consider a system for which the flow of matter is outward, so that its mass M is a monotonic decreasing function of the time. Such a system is represented in Figs. (6a) and (6b). The surface $ABCFDEA$ of Fig. (6a) represents the defining surface S for the time $t = t_1$. Since, when $t = t_1$, the material points which comprise the system S_2 are identically those which comprise the system S, we see that for this instant we may choose the defining surface S_2 to be identical with the surface S. In general, as the time t increases, the surface S will change in both position and form. For the time $t = t_1 + \epsilon$, where ϵ is a positive infinitesimal satisfying the inequality $\epsilon \leq b - t_1$, its form and position

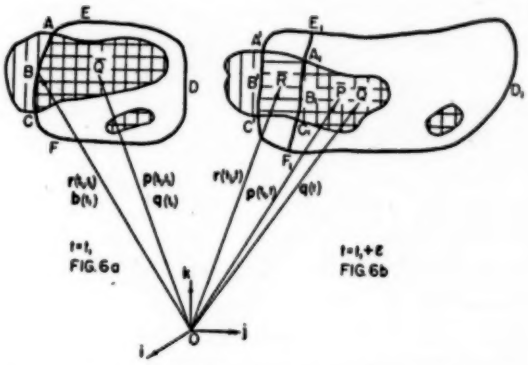

FIG. 6. System for which the flow of matter is outward through one region and the mass is a monotonic decreasing function of the time.

are represented by the surface $A_1B_1C_1F_1D_1E_1A_1$ of Fig. (6b). The region σ of the surface S corresponding to the times $t=t_1$ and $t=t_1+\epsilon$ is represented, respectively, by the surfaces ABC of Fig. (6a) and $A_1B_1C_1$ of Fig. (6b). Consider, now, the particular material points which, at the time $t=t_1$, coincide with the portion ABC of the surface S. At the end of the time interval ϵ these material points will, in general, occupy new positions. In their new locations in space they will define a surface which is represented in Fig. (6b) by the surface $A'B'C'$. This new surface need not, of course, be congruent with the surface ABC. Now an essential feature of any choice of the surface S_2 is that the material points which it includes at any time t of the interval $a\leq t\leq b$ must be identical with those which it includes at the particular time $t=t_1$. For the time $t=t_1+\epsilon$, therefore, the surface S_2 must be such that a portion of it is composed of the surface $A'B'C'$. With this restriction in mind we see that the surface $A'B'C'F_1D_1E_1A'$ of Fig. (6b) represents a suitable choice. In accordance with this choice the surface $A'B'C'F_1C_1B_1A_1E_1A'$ may be taken to represent the surface S_1. The remaining symbols in Figs. (6a) and (6b) have the same meanings as in the previous portions of this paper.

The next case we shall consider is that of a system S whose change of mass throughout the interval $a\leq t\leq b$ is caused by the simultaneous flow of matter through several regions of its defining surface. For the sake of simplicity we shall limit our discussion to a system for which (a), the number of such regions is two; (b), the flow of matter through both regions is outward; and (c), the regions are non-contiguous. The surface $ABCFKJGDHINEA$ of Fig. (7a) represents the defining surface S of such a system for the time $t=t_1$. Mass is leaving the system through the non-contiguous regions ABC and GDH. At a later time, $t_1+\epsilon$, the system S will have changed, in general, both its position and its form. The surface $A_1B_1C_1F_1K_1J_1G_1D_1H_1I_1N_1E_1A_1$ of Fig. (7b) represents the surface S in its new position and form. In this figure the regions through which mass is leaving the system are labelled $A_1B_1C_1$ and $G_1D_1H_1$. To obtain the translational equation of motion for a system of this type we may proceed as follows: Let a surface S_4 be chosen subject to the condition that throughout

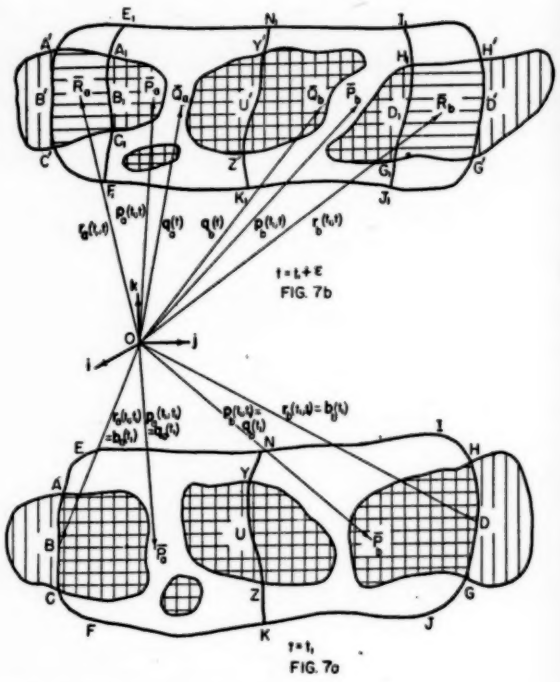

FIG. 7. System for which the flow of matter is outward through two regions and the mass is a monotonic decreasing function of the time.

the interval $a\leq t\leq b$ it must divide the system S into two systems S_a and S_b each of which is of the type previously considered. This restriction will be met if we require the set of those material points which lie in the surface S_4 at any time of the interval $a\leq t\leq b$ to be identical with the set of those particular points which lie in this surface at the instant t_1. In Fig. (7a) the surface $KZUYN$ represents such a surface S_4. At the end of a time interval ϵ, the particular material points which coincide with the region ZUY of this surface at the instant t_1 will have moved to new positions. The surface which they define in their new positions is represented by the surface $Z'U'Y'$ of Fig. (7b). If our restriction upon S_4 is to be met, it is necessary that at the time $t=t_1+\epsilon$ a portion of S_4 should be composed of the surface $Z'U'Y'$. Accordingly, a suitable choice of S_4 for this instant is represented by the surface $K_1Z'U'Y'N_1$. In order to distinguish between the various scalars and vectors which are associated with the systems S_a and S_b, we shall use the subscripts a and b, respectively. Thus, for example, the system of constant mass which becomes identical with the system S_a at the instant $t=t_1$ will be

denoted by the symbol $S_{2,a}$, while the corresponding system for the system S_b will be denoted by the symbol $S_{2,b}$. For the time $t=t_1$, S_a and $S_{2,a}$ are represented by the single surface $ABCFKZUYNEA$; S_b and $S_{2,b}$ by the single surface $KJGDHINYUZK$. The representation of the surfaces S_a, $S_{1,a}$, $S_{2,a}$, S_b, $S_{1,b}$, and $S_{2,b}$ for the time $t=t_1+\epsilon$ appears in Fig. (7b): S_a is represented by the surface $A_1B_1C_1F_1K_1Z'U'Y'N_1E_1A_1$,

$S_{1,a}$ by $A'B'C'F_1C_1B_1A_1E_1A'$,
$S_{2,a}$ by $A'B'C'F_1K_1Z'U'Y'N_1E_1A'$,
S_b by $K_1J_1G_1D_1H_1I_1N_1Y'U'Z'K_1$,
$S_{1,b}$ by $J_1G'D'H'I_1H_1D_1G_1J_1$,

and

$S_{2,b}$ by $K_1J_1G'D'H'I_1N_1Y'U'Z'K_1$.

Corresponding to the systems S_a and S_b, there will be two equations, each of the form (20). Thus, we shall have

$$\mathbf{F}_a(t)=\mathbf{L}_a'(t)+[\mathbf{u}_a(t)-2\mathbf{w}_a(t)]\cdot M_a'(t), \quad (a\leq t\leq b); \tag{55a}$$

$$\mathbf{F}_b(t)=\mathbf{L}_b'(t)+[\mathbf{u}_b(t)-2\mathbf{w}_b(t)]\cdot M_b'(t), \quad (a\leq t\leq b). \tag{55b}$$

We note now that in the summation $\mathbf{F}_a(t)$ of the external forces acting upon the system S_a there will appear the forces of reaction across the surface S_4. Reaction forces of like magnitude and direction but with opposite sense will appear in the summation $\mathbf{F}_b(t)$. Consequently, if we add together the corresponding sides of Eqs. (55a) and (55b), we shall find that the reaction forces do not appear in the resulting equation. For the various scalars and vectors we shall have the relations

$\mathbf{F}_a(t)+\mathbf{F}_b(t)=\mathbf{F}(t)$, the sum of the external forces on the system S; (56a)

$\mathbf{L}_a'(t)+\mathbf{L}_b'(t)=\mathbf{L}'(t)$, the time derivative of the linear momentum of S; (56b)

$M_a'(t)+M_b'(t)=M'(t)$, the time derivative of the mass of S; (56c)

$$\mathbf{u}_a(t)\cdot M_a'(t)+\mathbf{u}_b(t)\cdot M_b'(t)=\mathbf{u}(t)\cdot M'(t); \tag{56d}$$

and

$$\mathbf{w}_a(t)\cdot M_a'(t)+\mathbf{w}_b(t)\cdot M_b'(t)=\mathbf{w}(t)\cdot M'(t). \tag{56e}$$

The relations (56d) and (56e) are to be regarded as defining relations for the vectors $\mathbf{u}(t)$ and $\mathbf{w}(t)$ in this case. In view of these relations, the addition of the Eqs. (55a) and (55b) will lead to the result

$$\mathbf{F}(t)=\mathbf{L}'(t)+[\mathbf{u}(t)-2\mathbf{w}(t)]\cdot M'(t), \quad (a\leq t\leq b). \tag{57}$$

This, the translational equation of motion for this case, is in precisely the same form as the relation (20).

An analogous argument will lead to a rotational equation of motion of the form (26). Thus, we shall have

$$\mathbf{K}(t)=\mathbf{H}'(t)-\boldsymbol{\lambda}(t), \quad (a\leq t\leq b), \tag{58}$$

where, in this case,

$\mathbf{K}(t)=\mathbf{K}_a(t)+\mathbf{K}_b(t)$, the moment of the external forces on S about the fixed point J; (59a)

$\mathbf{H}'(t)=\mathbf{H}_a'(t)+\mathbf{H}_b'(t)$, the time derivative of the angular momentum of the system S relative to the point J; (59b)

and

$$\boldsymbol{\lambda}(t)\equiv\boldsymbol{\lambda}_a(t)+\boldsymbol{\lambda}_b(t). \tag{59c}$$

The relation (59c) is to be considered as a defining relation for the vector $\boldsymbol{\lambda}$ in this case. Systems for which the flow of matter is inward through some regions of the defining surface S and, simultaneously, outward through other regions may be treated in a similar manner.

I am indebted to Dr. H. T. Muhly for several helpful discussions; to Lt. E. E. Betz, and Dr. A. E. Currier for a critical reading of my manuscript.

Letters to the Editor

PROMPT publication of brief reports of important discoveries in physics may be secured by addressing them to this department. The closing date for this department is the third of the month. Because of the late closing date for the section no proof can be shown to authors. The Board of Editors does not hold itself responsible for the opinions expressed by the correspondents. Communications should not in general exceed 600 words in length.

The Theory of Diffraction

F. B. PIDDUCK
Corpus Christi College, Oxford, England
July 28, 1945

THE use of Kirchhoff's surface integral in the theory of diffraction has often been felt to be unsatisfactory, and many attempts at improvement have been made. The present state of the theory is described with references to Stratton.[1] These attempts, at the best, repair the deficiencies of the integral when the screen is perfectly absorbing or perfectly reflecting, and do not, I think, touch on the problem of a screen of any composition. Consideration of currents in sheets has led me to a more drastic process, valid when the wave-length is small.

Suppose that a wave falls obliquely on a sheet of small thickness d, and of dielectric constant ϵ and conductivity γ. If the wave-length is small, we can first solve the problem for an infinite sheet of thickness d and a plane wave, and then take the electric moments in the sheet as if they were finite and let them radiate like Hertzian oscillators. If γ is very great, the moments are all in a thin layer on the surface. In that case, a primary wave $A\cos(\omega t-kr_0)/r_0$ from P_0 (of any polarization) gives rise to a secondary wave $A\cos\varphi\sin(\omega t-kr-kr_0)dS/\lambda r\iota_0$ at Q, where dS is an element of the diffracting screen at P, φ the angle of incidence, $\iota_0=P_0P$, and $r=PQ$. This is Kirchhoff's formula in the most important case of direct vision, the only case in which it is confirmed. Consideration of space compels me to forego details, which will be found in a book on *Currents in Aerials and High Frequency Networks* to be published shortly by the Clarendon Press, Oxford. If we have a small hole instead of a screen, and a plane wave, the current per meter in the perforated sheet is the same as in the hole. The electrical effect of the two is nearly that of a complete sheet, which below the sheet is equal and opposite to that of the incident light. This is Babinet's principle, a natural consequence of the smallness of the wave-length. I have investigated the diffraction of a sheet of dielectric constant ϵ and conductivity γ at any angle, but the results are complicated. In treating the problem this way we are treating the physical phenomenon as it is, and determining the electrical state of a diffracting screen at all points of it. Such a spoint of view must, I think, ultimately replace the delicate and restricted methods based on Kirchhoff's integral.

[1] Stratton, *Electromagnetic Theory* (McGraw-Hill Book Company, Inc., New York, 1941) pp. 460–70.

Hρ-Distribution of Fission Fragments

N. O. LASSEN
Institute of Theoretical Physics, University of Copenhagen, Copenhagen, Denmark
June 16, 1945

AS was reported earlier,[1] the total charge of fission fragments has been determined by deflecting the fragments from a thin layer of uranium in the magnetic field of the Copenhagen cyclotron. The uranium was placed inside the cyclotron about 6 mm behind an internal target of beryllium which was bombarded by 6 Mev deuterons, thus being a strong source of neutrons. The dimensions of the uranium layer were: width 1.0 mm, length 20 mm, thickness 0.35 mg/cm²; it was placed parallel to the lines of the magnetic force and the fragments used were emitted nearly normally from the surface. They passed through a slit S_1 of variable width placed 10 cm from the uranium layer and through a second slit S_2 10 cm further away; the latter had a fixed width of 3.0 mm and was covered by a foil of thickness 0.79 mg/cm² of mica and 0.25 mg/cm² of aluminium through which the particles entered into an ionization chamber filled with pure argon. The collecting electrode of the chamber was connected to a linear amplifier and this in turn to a cathode-ray oscillograph, which was photographed on a moving film. The slit S_1 could be moved in a direction normal to the plane determined by the uranium layer and the window S_2; the various positions of this slit then allowed particles with various values of Hρ to pass from the uranium layer to the ionization chamber. For all positions of the slit was seen a background consisting of a great number of pulses due to recoiling argon atoms in the ionization chamber; but only when the slit S_1 was displaced between 7 and 14 mm from the plane through the layer and the mica window S_2 pulses of much higher energy corresponding to fission fragments occurred.

As more fully reported,[1] the Hρ-distribution curve for

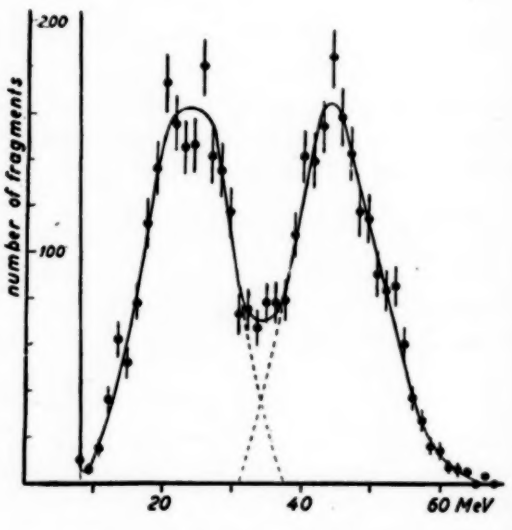

FIG. 1. Energy distribution of fission fragments having traversed 0.79 mg/cm² of mica.

the fission fragments was determined in this way. Later on, small improvements of the apparatus have made it possible to measure the $H\rho$-distribution for each of the two groups of fission fragments separately.

Figure 1 shows the energy distribution as obtained when

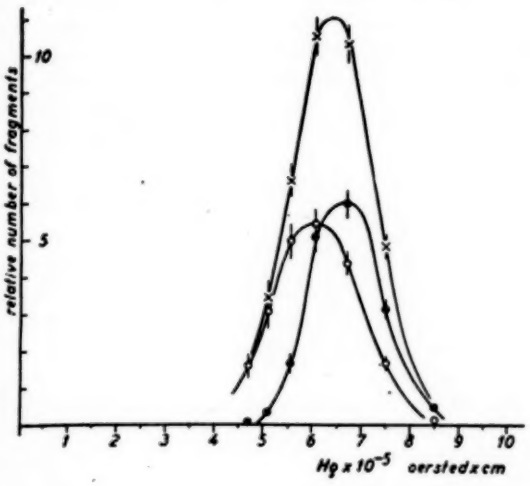

FIG. 2. $H\rho$-distribution of fission fragments. Full circles: light group. Open circles: heavy group. Crosses: Both groups.

the slit S_1 was made so wide (7 mm) that the fission fragments entering through S_2 could have all possible values of $H\rho$. The figure clearly shows that, apart from a very few exceptions, the pulses of energies higher than 34 Mev are caused by fragments of the light, most energetic group, while the fragments of the heavy group correspond to pulses between 9 and 34 Mev; pulses of energies lower than 10 Mev are caused by coincidences between recoiling argon atoms. In the $H\rho$-measurements the slit S_1 had a width of 1.0 mm and it was moved in steps of 1.0 mm; for the different positions of S_1 the number of fragments were counted, of course for equal neutron doses, and by means of the photographic record divided into two groups corresponding to the sizes of the pulses. In this way we get the number of fragments of each group as a function of the displacement of S_1 and we then calculate by means of the known magnetic field (which is not homogeneous) the $H\rho$-distribution curves shown on Fig. 2.

As seen, the two groups have nearly the same values of $H\rho$, but the light group has evidently slightly higher $H\rho$-values than the heavy one. Putting the most frequent value of mE to 8.5×10^3 mass units$\times$Mev[1] we get for the total charge of the light and the heavy group 20ϵ and 22ϵ, respectively, when ϵ denotes the electronic charge. This is in agreement with calculations by Professor Bohr[2] which predict an effective charge of fission fragments of about 20ϵ; yet the agreement is not perfect, as the theory involves a higher effective charge of the light group than of the heavy one in contradiction to the present experiments. Nevertheless, it is no real disagreement; as pointed out by Professor Bohr in the paper, the total fragment charge need not be identical with the charge effective in electronic interactions.

The author wishes to express his heartiest thanks to the Director of the Institute of Theoretical Physics, Professor Niels Bohr, and to Professor J. C. Jacobsen for their interest in the work and their great encouragement.

[1] N. O. Lassen, Kgl. Danske Vid. Sels. Math.-Fys. Medd. 22, No. 2 (1945). In press.
[2] Niels Bohr, Phys. Rev. 59, 270 (1941).

The Synchrotron—A Proposed High Energy Particle Accelerator

EDWIN M. MCMILLAN
University of California, Berkeley, California
September 5, 1945

ONE of the most successful methods for accelerating charged particles to very high energies involves the repeated application of an oscillating electric field, as in the cyclotron. If a very large number of individual accelerations is required, there may be difficulty in keeping the particles in step with the electric field. In the case of the cyclotron this difficulty appears when the relativistic mass change causes an appreciable variation in the angular velocity of the particles.

The device proposed here makes use of a "phase stability" possessed by certain orbits in a cyclotron. Consider, for example, a particle whose energy is such that its angular velocity is just right to match the frequency of the electric field. This will be called the equilibrium energy. Suppose further that the particle crosses the accelerating gaps just as the electric field passes through zero, changing in such a sense that an earlier arrival of the particle would result in an acceleration. This orbit is obviously stationary. To show that it is stable, suppose that a displacement in phase is made such that the particle arrives at the gaps too early. It is then accelerated; the increase in energy causes a decrease in angular velocity, which makes the time of arrival tend to become later. A similar argument shows that a change of energy from the equilibrium value tends to correct itself. These displaced orbits will continue to oscillate, with both phase and energy varying about their equilibrium values.

In order to accelerate the particles it is now necessary to change the value of the equilibrium energy, which can be done by varying either the magnetic field or the frequency. While the equilibrium energy is changing, the phase of the motion will shift ahead just enough to provide the necessary accelerating force; the similarity of this behavior to that of a synchronous motor suggested the name of the device.

The equations describing the phase and energy variations have been derived by taking into account time variation of both magnetic field and frequency, acceleration by the "betatron effect" (rate of change of flux), variation of the latter with orbit radius during the oscillations, and energy losses by ionization or radiation. It was assumed that the period of the phase oscillations is long compared to the period of orbital motion. The charge was taken to be one electronic charge. Equation (1) defines the equilib-

rium energy; (2) gives the instantaneous energy in terms of the equilibrium value and the phase variation, and (3) is the "equation of motion" for the phase. Equation (4) determines the radius of the orbit.

$$E_0=(300cH)/(2\pi f), \tag{1}$$

$$E=E_0[1-(d\phi)/(d\theta)], \tag{2}$$

$$2\pi\frac{d}{d\theta}\left(E_0\frac{d\phi}{d\theta}\right)+V\sin\phi =\left[\frac{1}{f}\frac{dE_0}{dt}-\frac{300}{c}\frac{dF_0}{dt}+L\right]+\left[\frac{E_0}{f^2}\frac{df}{dt}\right]\frac{d\phi}{d\theta}, \tag{3}$$

$$R=(E^2-E_r^2)^{\frac{1}{2}}/300H. \tag{4}$$

The symbols are:

E = total energy of particle (kinetic plus rest energy),
E_0 = equilibrium value of E,
E_r = rest energy,
V = energy gain per turn from electric field, at most favorable phase for acceleration,
L = loss of energy per turn from ionization and radiation,
H = magnetic field at orbit,
F_0 = magnetic flux through equilibrium orbit,
ϕ = phase of particle (angular position with respect to gap when electric field = 0),
θ = angular displacement of particle,
f = frequency of electric field,
c = light velocity,
R = radius of orbit.

(Energies are in electron volts, magnetic quantities in e.m.u., angles in radians, other quantities in c.g.s. units.)

Equation (3) is seen to be identical with the equation of motion of a pendulum of unrestricted amplitude, the terms on the right representing a constant torque and a damping force. The phase variation is, therefore, oscillatory so long as the amplitude is not too great, the allowable amplitude being $\pm\pi$ when the first bracket on the right is zero, and vanishing when that bracket is equal to V. According to the adiabatic theorem, the amplitude will diminish as the inverse fourth root of E_0, since E_0 occupies the role of a slowly varying mass in the first term of the equation; if the frequency is diminished, the last term on the right furnishes additional damping.

The application of the method will depend on the type of particles to be accelerated, since the initial energy will in any case be near the rest energy. In the case of electrons, E_0 will vary during the acceleration by a large factor. It is not practical at present to vary the frequency by such a large factor, so one would choose to vary H, which has the additional advantage that the orbit approaches a constant radius. In the case of heavy particles E_0 will vary much less; for example, in the acceleration of protons to 300 Mev it changes by 30 percent. Thus it may be practical to vary the frequency for heavy particle acceleration.

A possible design for a 300 Mev electron accelerator is outlined below:

peak H = 10,000 gauss,
final radius of orbit = 100 cm,
frequency = 48 megacycles/sec.,
injection energy = 300 kv,
initial radius of orbit = 78 cm.

Since the radius expands 22 cm during the acceleration, the magnetic field needs to cover only a ring of this width, with of course some additional width to shape the field properly. The field should decrease with radius slightly in order to give radial and axial stability to the orbits. The total magnetic flux is about $\frac{1}{3}$ of what would be needed to satisfy the betatron flux condition for the same final energy.

The voltage needed on the accelerating electrodes depends on the rate of change of the magnetic field. If the magnet is excited at 60 cycles, the peak value of $(1/f)(dE_0/dt)$ is 2300 volts. (The betatron term containing dF_0/dt is about $\frac{1}{3}$ of this and will be neglected.) If we let V = 10,000 volts, the greatest phase shift will be 13°. The number of turns per phase oscillation will vary from 22 to 440 during the acceleration. The relative variation of E_0 during one period of the phase oscillation will be 6.3 percent at the time of injection, and will then diminish. Therefore, the assumptions of slow variation during a period used in deriving the equations are valid. The energy loss by radiation is discussed in the letter following this, and is shown not to be serious in the above case.

The application to heavy particles will not be discussed in detail, but it seems probable that the best method will be the variation of frequency. Since this variation does not have to be extremely rapid, it could be accomplished by means of motor-driven mechanical turning devices.

The synchrotron offers the possibility of reaching energies in the billion-volt range with either electrons or heavy particles; in the former case, it will accomplish this end at a smaller cost in materials and power than the betatron; in the latter, it lacks the relativistic energy limit of the cyclotron.

Construction of a 300-Mev electron accelerator using the above principle at the Radiation Laboratory of the University of California at Berkeley is now being planned.

Radiation from a Group of Electrons Moving in a Circular Orbit

EDWIN M. MCMILLAN
University of California, Berkeley, California
September 9, 1945

A SINGLE electron of total energy E (rest energy $= E_r$) moving in a circle of radius R, radiates energy at the rate L (electron volts per turn), given by:

$$L=400\pi(e/R)(E/E_r)^4, \tag{1}$$

where e is the electronic charge in e.s.u., and $E>>E_r$. In the synchrotron one has the case of a rather concentrated group of electrons moving in the orbit, and the total amount of radiation depends on the coherence between the waves emitted by the individual electrons. For example, if there were complete coherence, the radiation per electron would be N times that given by (1), where N is the number of electrons in the group.

It is apparent from the above that an answer to the coherence problem is very important for any device in which groups of electrons are made to move in a circle with high velocity. This answer is given by a formula due to J. Schwinger (communicated to the author by I. I. Rabi). Schwinger's formula gives the radiation in each harmonic of the period of revolution, in a form that allows easy computation for any distribution of electrons around the orbit. It leads to the following conclusions:

(a) Most of the energy in (1) lies in very high harmonics.
(b) The coherence between the high harmonics from different electrons tends to become very small if the group has an appreciable angular spread.
(c) The low harmonics are partially coherent, and give an energy loss per electron per turn (L') depending on N, but not on E if $E>>E_r$.
(d) Because of fluctuations from a uniform distribution, each electron also radiates the same amount L that it would if alone in the orbit. The total radiation per electron is thus $L+L'$.

Values of L' have been computed numerically from Schwinger's formula for the case of N electrons covering uniformly an arc with an angular extent which is $1/m$ of a circle. This was done for $m=2$, 4, and 6; also the asymptotic form for large m was obtained. These values can all be fitted within a few percent by the formula:

$$L'\sim 400\pi(e/R)\times 2.4(m^{4/3}-1)N. \quad (2)$$

Applying (1) and (2) to the case where $R=100$ cm, $E/E_r=600$, $N=10^{11}$ (1/60 microcoulomb, giving 1 microampere at a 60 cycle repetition rate), and $m=6$, we get:

$$L=780 \text{ volts}, \quad L'=1400 \text{ volts}.$$

Thus the radiation loss will not seriously affect the operation of the synchrotron. Furthermore, L. I. Schiff has shown that the coherent part L', which is mostly in the very low harmonics, can be strongly reduced by shielding.

A Note on the Separation of Gases by Diffusion into a Fast-Streaming Vapor

F. A. SCHWERTZ
*Mellon Institute of Industrial Research, Pittsburgh, Pennsylvania**
December 8, 1944

WHILE it is well known that gas mixtures may be separated by diffusion into a fast-streaming vapor, the potential speed of the process is not generally appreciated. The simple calculation given below may serve to correct this situation. The calculation is meant to be illustrative and not quantitative in the sense that it would agree with experimental data.

In Fig. 1, A and B are two channels connected by a cross-duct, C, of very small cross-sectional area. A pure gas is assumed to be traveling in A at a high velocity in the downward direction. Similarly, a vapor is flowing in B. The pressure differential across C is assumed to be such that the fluid velocity in the x direction is constant. To express the rate of transfer of the gas the equation:

$$\mathbf{i}=\rho\mathbf{v}-D \text{ grad } \rho \quad (1)$$

may be used.[1] In this equation $\mathbf{i}$ is the rate of gas transfer per unit area; ρ, the density of the gas; $\mathbf{v}$, the fluid velocity; and D, the mutual coefficient of diffusion of gas and vapor. For the steady state div $\mathbf{i}=0$, so that

$$\text{div } (\rho\mathbf{v})-D \text{ div grad } \rho=0. \quad (2)$$

TABLE I. Rate of diffusion, i, of H_2 into water vapor. (i is expressed in cm³/cm²×sec. at 150°C and 1 atmos.)

v (cm/sec.)	$b=0.01$ cm	$b=0.1$ cm	$b=1.0$ cm
−1000	2.34	000	000
−100	120	0.234	000
−10	156	12.0	0.023
−1	164	15.6	1.20
0	165	16.5	1.65
+1	166	17.6	2.20
+10	177	22.0	10.0
+100	220	100	100
+1000	1002	1000	1000

TABLE II. Separation currents and compositions. (i is expressed in cm³/cm²×sec. at 150°C and 1 atmos.)

v	$b=0.01$ cm		$b=0.1$ cm		$b=1.0$ cm	
cm/sec.	i	f_{H_2}	i	f_{H_2}	i	f_{H_2}
−1000	1.17	1.00	000	—	000	—
−100	62.3	0.964	0.117	1.00	000	—
−10	91.5	0.852	6.23	0.964	0.012	1.00
−1	97.8	0.839	9.15	0.852	0.623	0.963
0	98.5	0.837	9.85	0.837	0.985	0.837
+1	99.3	0.836	107	0.826	1.63	0.678
+10	107	0.827	16.3	0.678	10.0	0.500
+100	162	0.678	100	0.500	100	0.500
+1000	1001	0.500	1000	0.500	1000	0.500

If ρ is considered a function of x only, and $v_x=v$ is considered constant, then

$$\frac{\partial^2\rho}{\partial x^2}-\frac{v}{D}\frac{\partial\rho}{\partial x}=0. \quad (3)$$

If it is further assumed that the velocities in A and B are so large that the concentration of gas in B and of the vapor in A are substantially zero, (3) must be solved subject to the boundary conditions:

$$\rho(x)=\rho_0 \quad \text{at} \quad x=0,$$

and

$$\rho(x)=0 \quad \text{at} \quad x=b.$$

The result is

$$\rho=\rho_0[e^{vx/D}-e^{vb/D}]/[1-e^{vb/D}]. \quad (4)$$

For the current (1) gives

$$i=\rho_0 v/[1-e^{-vb/D}]. \quad (5)$$

The limit of i as v approaches zero is

$$i_0=\rho_0 D/b. \quad (6)$$

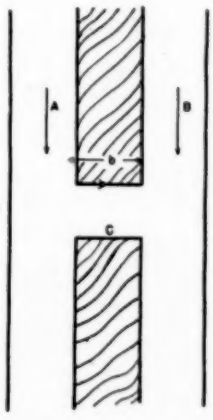

FIG. 1. Gas and vapor streaming by a connecting duct.

In Table I the calculated values of i for the diffusion of hydrogen into water vapor are presented for $D=1.65$ cm²/sec. at 150°C.

The value of i for $b=0.01$ cm and $v=0$ corresponds to 19,500 cu. ft. of hydrogen per square foot per hour.

If now it is assumed that two gases will diffuse independently of one another, the ratio of the currents will be

$$\frac{i_2}{i_1}=\frac{\rho_{0,2}[1-\exp(-vb/D_1)]}{\rho_{0,1}[1-\exp(-vb/D_2)]} \tag{7}$$

and the fraction, f_1, of the first gas in the separated portion will be

$$f_1=\left\{1+\frac{\rho_{0,2}[1-\exp(-vb/D_1)]}{\rho_{0,1}[1-\exp(-vb/D_2)]}\right\}^{-1}.$$

In Table II the values of i and $f_1=f_{H_2}$ are given for a gas mixture originally containing 50 percent H_2 and 50 percent CO_2. $D=0.32$ cm²/sec. was used for the mutual coefficient of diffusion of CO_2 and water vapor.

Table II shows that, at a fixed value of v, an increase in H_2 concentration may be effected merely by increasing the length, b, of the cross-duct, but only at the cost of a severe reduction in the gas current.

The calculations suggest that a thin, perforated metal sheet would serve as the nucleus of an effective gas separator.[2]

* Industrial Fellowship on Coke-Plant Physical Technology sustained by The Koppers Company.

[1] G. Hertz, Physik. Zeits. **23**, 433 (1922); Proc. Acad. Sci. Amsterdam **25**, 434 (1922).

[2] C. G. Maier, Bureau of Mines Bulletin 431.